Motion of the Foot Inside a Hockey Skate: As Measured from Bone, Skin, and Skate Markers

By

©Mouafak Al Hadi

Thesis submitted in partial fulfillment
of the degree of Masters of Science in Anatomy & Neurobiology

May 2001

Department of Cellular & Molecular Medicine

University of Ottawa

ABSTRACT

In filming and digitizing human segmental motion, external markers do not necessarily represent a true picture of the actual bone movement. When surface markers are placed on the skin or skate boot (in ice hockey) they move according to skin or boot movement, which does not exactly match bone movement. This results in a misrepresentation of the joint axes of rotation and a greater margin of error in motion measurement and analysis. This problem occurs for ankle and foot movements as their motion is quantified about the ankle joint complex (talocrural and subtalar joints).

Variability amongst bone, skin, and shoe markers has been identified in the works of Reinschmidt (1997). He concluded that markers placed on the shoe tend to overestimate tibiocalcaneal rotations. However, hockey skates are vastly more rigid than regular shoes and their restriction of foot movement is greater. Therefore, shoes and hockey skates cannot be considered identical. The present study aims at exploring differences amongst bone, skin, and skate marker based motions of the foot during skating

Three holes were made in a right hockey skate above the tarsal bones, and three plastic screws with lead markers were attached to a piece of thermoplastic molded to the area of the skin below the holes. The lead markers protruded from the skate. Three other lead markers were attached to the skate boot. Eight subjects participated in the experiment where the foot inside the skate was x-rayed within a calibration cage with lead markers embedded in its sides. Two x-ray shots with 30° angle between them were

taken of the still foot in each of three different positions; full dorsiflexion, neutral, and full plantar flexion with 45° of external rotation. Three bony landmarks were established on the tarsal bones in each image. The lead markers and the three bony landmarks were digitized using Ariel Performance Analysis System. The subject then performed several trials of forward skating on ice while being filmed by two high speed (200 Hz; resolution 740X256 pixels) video cameras that were mounted on platform tracking the subject along the line of skating. Skin and skate markers were also digitized on the video views using Ariel Performance Analysis System.

The three dimensional positions of the centroids of each type of markers (bone, skin, skate) were determined on the x-rays at every foot position (dorsiflexion, neutral, and plantar flexion). The positions of skin and skate centroids were also determined on the video views along the motion from heel-off to toe-off. The motions of the different types of markers were compared to each other by calculating the change in inter-centroid distances. On the x-ray images, a vector that passes through two markers on the bone, a vector that passes through two markers on the skin, and a vector that passes through two markers on the skate were used to represent foot rotations from dorsiflexion to neutral position and from neutral position to plantar flexion based on bone, skin, and skate markers. Foot rotations on the video views were determined by calculating the rotations of a vector that passes through two skin markers and a vector that passes through two skate markers from heel-off to toe-off. Paired samples t-tests were used to compare the rotations of different vectors to each other.

The results showed that a significant difference amongst bone, skin, and skate rotations existed during plantar flexion but not during dorsiflexion. This significant difference extended to the total motion from dorsiflexion to plantar flexion where skate rotations were 26% smaller than bone rotations and 49% smaller than skin rotations. Bone rotations were 31% smaller than skin rotations. Indicating that the motion of the bone is overestimated by the motion of the skin and underestimated by the motion of the skate. During actual skating, skate rotations were 22% smaller than skin rotations, but the difference was not significant. All three motions exhibited a similar pattern and the difference between skate and bone rotations from neutral position to plantar flexion and from dorsiflexion to plantar flexion was systematic across all subjects except one.

Based on the results of this study, it can be concluded that, unlike shoe motion, the rigidity of the skate structure causes the skate motion to underestimate the motion of the underlying bony and skin structures. However, it is not clear whether this difference exists in movements other than planatr/dorsiflexion around the ankle joint complex. It is also evident from the results that the general pattern of skate motion does accurately represent the pattern of bone and skin motions since the trends of all three motions are similar and a predictive relationship might be present between skate and bone motions.

DEDICATION

To my parents, Linda and Hamad Al Hadi, and to my whole family, the infinite source of inspiration...

ACKNOWLEDGMENTS

I would like to express my gratitude and deep appreciation to the following individuals who contributed to making this project a success.

- Dr. Mario Lamontagne for his guidance, help, and support through out the project.
- Dr. Max Hincke for his guidance, professionalism and patience.
- Dr. Pierre Fortier for his support and understanding.
- Dr. Heidi Sveistrup for providing valuable advice and Dr. Gord Robertson for his guidance and help.
- Dr. Pete Stothart for being a good friend and mentor.
- My friend Jason Carey P. Eng for lending his wonderful designing skills.
- My friends and colleagues at the BHRL; Dany Lafontaine, Marshal Kendall, Dr. Norman Murphy, Sebastien Delorme, Dan Theoret.
- My friends Ismael El Mach and Yan Lamontagne for their brilliant minds and willingness to help.
- Mr. Micheal Guzzo for his great work on the x-ray and his dedication and honesty.
- My deepest love and gratefulness to my partner and friend Nira whose patience and unwavering support were the reasons this project was completed.

TABLE OF CONTENTS

LIST OF TABLES

LIST OF FIGURES

INTRODUCTION

In recent years, three-dimensional analysis of human movement has witnessed an explosion in application where it has entered a diverse array of fields such as medicine, ergonomics, and sport performance. Three-dimensional analysis of pathological gait is a very important tool for clinicians in the diagnosis and assessment of conditions ranging from cerebral palsy, stroke, and Parkinson's, to various orthopaedic disorders. Accurate description of body motions in space is essential for understanding the workings of the locomotion system. This understanding is important for the improvement of subnormal and even normal activity in sports or rehabilitation settings. It also provides valuable clues on how to enhance workspace design. (Allard, Stokes, and Blanchi, 1995) The potential of this method of analysis of motion is tremendous and still has plenty of room for improvement and development.

Stereophotogrammetry and stereoradiography are two of the most common techniques used in three-dimensional analysis of motion. Photogrammetric techniques rely mainly on skin and shoe markers to represent body segments while joint axes of rotation are determined by bony landmarks. The 3-D motion is reconstructed from two or more camera images using algorithms such as the Direct Linear Transformation (Abdel-aziz and Karara, 1971). The problem with these techniques is that they do not take into account the difference between skin/shoe motion and the motion of the underlying bone. The relative movement between skin/shoe and bone results in the misrepresentation of the joint axis of rotation and introduces errors in motion measurements.

Steroeradiographic measurements of motion are obtained in a way analogous to photogrammetry through the use of two x-ray images of the segment, which eliminates the need for external (skin/shoe) markers and allows representation of actual bone motion. However, the use of x-rays is constrained with issues of dosage and the inability to film continuous motion, in addition to the difficulty of identifying bony landmarks that are identical in more than one image.

Researchers have developed various techniques in order to overcome problems inherent in the two methods. The problem of using external markers to represent segment motion could be avoided by directly measuring skeletal motion through the use of bone pins (Reinschmidt, 1997; La Fortune et al, 1994) or external fixation devices that aim at limiting the movement of the skin (Cappozzo et al, 1996). In stereoradiography researchers used bone implanted metal (tantalum) markers as landmarks. However, the application of these methods remains limited due to their invasiveness. Therefore, the use of skin/shoe markers remains the easiest and most accessible method for three-dimensional reconstruction of motion. This fact underlines the need for knowledge about the difference and relationship between skin/shoe movement and the underlying bone movement, in order to correctly interpret external marker-based data.

Variability amongst bone, skin, and shoe markers has been identified in the works of Reinschmidt (1997). He concluded that markers placed on the shoe tend to overestimate tibiocalcaneal angles. However, in the case of skate boots, the restriction of the foot movement is greater than in the shoes due to the high stiffness of hockey skates.

The present study aims at exploring the difference between motion measured by bone and skin markers and motion measured by skate boot surface markers.

Objectives

The main purpose of the study is to explore how accurately skate motion represents the motion of the underlying bone. This purpose will be achieved through the following objectives:

1- To explore the difference between three-dimensional motions calculated from each type of marker (bone, skin, skate).

2- To calculate the angles between foot positions during a simulated push-off movement in skating based on bone, skin, and skate markers, and during a real push-off movement based on skin and skate markers.

3- To compare foot rotations based on each type of marker.

Objective 1 will be achieved through calculating the three-dimensional positions of the centroid of each type of markers (skin, bone, skate) at three different positions of the foot; dorsiflexion, neutral, and plantar flexion. In Addition, the positions of the centroid of skin and skate markers will also be calculated at heel-off and toe-off positions during a real skating motion on ice. Objective 2 will be achieved through calculating the three-dimensional rotations of a vector passing through two markers on the foot along a push-off motion. These rotations will be determined at three different positions *in-vivo* (dorsiflexion, neutral, and plantar flexion) and at heel-off and toe-off positions on ice. Objective 3 will be achieved through comparing the magnitudes of foot rotations obtained from the different types of markers at the above-mentioned positions.

Relevance

Kinematic analyses of lower extremities during skating treat the foot as a rigid segment. They also use markers that are placed on the skate boot relying on the assumption that foot motion is well represented by the skate motion. However, this assumption has not been tested or proven to be true. The results of this project will show how well externally measured kinematics represent the actual foot kinematics inside the skate boot. The knowledge gained by this project will help in understanding results obtained by previous studies that used boot markers. Information about error due to boot movement artefact will also help in the design of future studies that use boot markers. The methodology used in this study could be utilized to explore the behaviour of the foot inside footwear, which would help in providing a better view of design flaws and needs.

Statement of the problem

Current kinematic studies of the lower extremities during skating use markers that are mounted externally on the skate boot to represent the movement of the foot. This means that boot movement is considered to be identical to the movement of the bony segments of the foot. However, it has been shown that skin and shoes present an artefact that distorts the actual movement and results in a misinterpretation of results. The boot movement during skating might represent only the boot movement. This study will explore the difference between the actual movement of the foot and the movement of the boot.

Hypothesis

During skating, the motions of the skate boot do not truly represent the motions of the foot. There is a detectable difference between the two motions.

Rationale

Studies that examined skin and shoe artefact proved that the actual motion of the foot could be overestimated. This provides for a reasonable doubt against relying on the skate boot motion to represent actual foot motion. The stiffness of the skate boot and the fact that the foot is able to slightly move inside it as a result of voluntary motion, are indications that a discrepancy could exist between the two motions. Shoe and hockey skate artefacts cannot be considered identical due to the fact that the skate is considerably stiffer than the shoe, and it greatly restricts the motion around the ankle joint especially in plantar flexion as a result of the Achilles tendon guard (Kirchner, 1986).

DEFINITIONS

Ankle Joint Complex: is the term used to denote the combination of two joints: the talocrural joint between the tibia, fibula, and the talus; and the subtalar joint between the talus and the calcaneus.

Rotation: is used in this document to indicate the angle between different foot positions. In the x-ray part: the angle between the foot at dorsiflexion and the foot at neutral position, the angle between the foot at neutral position and the foot at plantar flexion, and the angle between the foot at dorsiflexion and the foot at plantar flexion are defined as: the rotation of the foot from dorsiflexion to neutral position, the rotation of the foot from neutral position to plantar flexion, and the rotation of the foot from dorsiflexion to plantar flexion respectively. For the on ice part, the term rotation means the angle between foot position at heel-of and foot position at toe-off.

REVIEW OF LITERATURE

The review of the literature will be divided into three parts. In the first part, the anatomical structures of and motions at the ankle, subtalar, and transverse tarsal joints will be summarised. In the second part, the kinematics of hockey as it pertains to the lower extremity will be discussed. The third and final part will deal with the three-dimensional reconstruction technique, Direct Linear Transformation.

Ankle joint

Structure

Ankle joint is the term used to refer to the talocrural joint: that is, the articulation of the tibia, fibula, and the talus. The tibia is located on the medial side of the leg and is the main weight bearing bone in the leg. The medial distal end of the tibia forms the medial malleolus. The fibula is the thin long bone along the lateral side of the tibia. Its distal end forms the lateral malleolus, which is located inferior and posterior in relation to the medial malleolus. The talus is the second largest of the tarsal bones and is located at the distal end of the ankle joint (Figure 1).

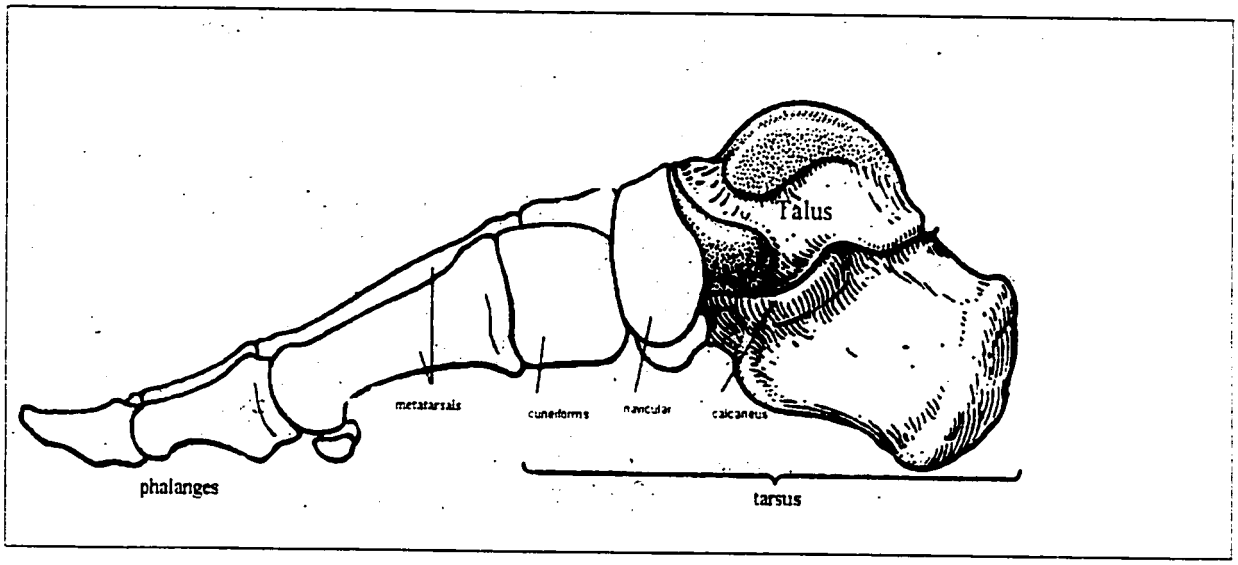

Figure 1. Bones of the foot, medial view of the right foot (Feneis, 1981)

The proximal segment of the ankle joint is formed by the concave surface of the distal tibia and the tibial and the fibular malleoli. These three surfaces together form a concave structure called the mortise. This mortise acts like the gripping part of an adjustable wrench. It provides both stability and mobility, and it relies on the proximal and distal tibiofibular joints for control of the changes in its size (Norkin & Levangie, 1992).

The distal segment of the ankle joint is formed by the body of the talus. It has three articular surfaces: lateral, medial, and superior facets. The superior facet is also called the trochlea. The trochlear surface is convex antero-posteriorly and concave medio-laterally (Rockar, 1995). The body of the talus has a wedge shape. It is wider anteriorly than posteriorly. The difference in width between front and back could reach 25% (Norkin & Levangie, 1992).

The stability of the mortise of the ankle joint is dependent on several ligaments. These are the crural tibiofibular interosseous ligament, the tibiofibular interosseous membrane, and the anterior and posterior tibiofibular ligaments. The tibiofibular ligaments control the mortise's grip on the body of the talus (Norkin & Levangie, 1992).

The capsule of the ankle joint is weak and thin. Therefore, two major ligaments maintain the stability; the deltoid ligament and the lateral collateral ligament. The deltoid ligament is a strong triangular ligament on the medial side of the ankle joint. Its fibers originate on the medial malleolus and insert on the navicular, the talus and the calcaneus. The deltoid ligament prevents the medial dislocation of the ankle joint and controls the motion at the extremes of range of motion. The lateral collateral ligament consists of three ligaments; the calcaneofibular ligament, and the posterior and anterior talofibular ligaments. The lateral collateral ligaments prevent the lateral dislocation of the ankle joint and controls motion at the extreme ends of the range of motion. The posterior talofibular ligament is the strongest of the lateral ligaments and is very seldom torn on its own, while the anterior talofibular ligament is the weakest and the most commonly torn. (Moore, 1992) and (Norkin & Levangie, 1992).

Function

The major motions at the ankle joint are considered to be dorsiflexion and plantar flexion. Dorsiflexion is the motion of the dorsum of the foot closer to the tibia. Plantar flexion is the motion of the dorsum of the foot away from the tibia. When the foot is fixed these two motions could take place through the movement of the shank close to or away from the dorsum of the foot. Some investigators have found that other motions,

such as in/eversion and external/internal rotation, take place at the ankle joint (Lundberg, 1988). However, the motions of the dorsi/plantar flexion predominate, and the contribution of the ankle joint to motions such as in/eversion and internal/external rotation is minimal compared to the contribution of the subtalar joint (Siegler, Chen, Schneck, 1988).

The joint axis of rotation at the ankle passes through the lateral malleolus, the body of the talus, and below the medial malleolus (Lundberg, 1988). However, the malleoli are not aligned due to the lateral twist of the distal end of the tibia and the position of the fibular malleolus more distally than the tibial one. Therefore, the axis of rotation is rotated 20 to 30° laterally in the transverse plane and inclined 10° down at the lateral malleolus. The range of motion at the ankle joint is commonly reported to be 20° of dorsiflexion and 30 to 50° of plantar flexion from the neutral position, which is the position of the foot at a right angle with the shank. The tilt in the ankle joint axis causes dorsi and plantar flexion motions to take place in two planes. Therefore, dorsiflexion is accompanied by a toe-out motion, and a toe-in motion accompanies plantar flexion (Norkin & Levangie, 1992).

The Subtalar Joint

Structure

The subtalar joint is the articulation between the talus superiorly and the calcaneus inferiorly. It is also called the talocalcaneal articulation (Rockar, 1995). The inferior surface of the talus rests on the dorsal aspect of the calcaneus. Its facets are two of the four facets on the inferior aspect of the talus. A large concave posterior facet articulates with the calcaneus, a middle facet (sometimes considered part of the head of talus), which articulates with the sustentaculum tali on the calcaneus and is separated from the posterior surface by sulcus tali. Sulcus tali is a groove for the ligaments connecting the talus and the calcaneus.

The calcaneus is the largest and the first to ossify of the foot bones. It is rectangular in shape and provides firm, elastic support for body weight as it is transferred to the talus through the tibia. The calcaneus also acts as lever for the calf muscles through its posterior projection beyond the leg bones (Rockar, 1995). It articulates with the talus superiorly and the cuboid anteriorly. The superior surface, which articulates with the talus, is divided into two parts. The anterior part is articular and is divided into three facets. The posterior part (non-articular) is convex medio-laterally and concave antero-posteriorly.

The subtalar joint has, within it and around it, an extensive ligament and soft tissue support. It is a synovial joint, surrounded by a weak joint capsule. The capsule is supported by the medial, lateral, and posterior talocalcaneal ligaments. Other ligaments include the interosseous talocalcaneal ligament (ligament of the tarsal canal), the cervical

and deltoid ligaments. The interosseous talocalcaneal ligament is a flat, oblique band, which originates in the tarsal canal. The fibers are directed upward and medially and insert into the sulcus of the talus. This ligament -together with the lateral, posterior and cervical ligaments- provides stability for the joint without obstructing rotation and translation. The interosseous talocalcaneal ligament is shorter than the more externally positioned cervical ligament. This allows the talus to pivot around the short ligaments until the cervical ligament is tensed (Figure, 2).

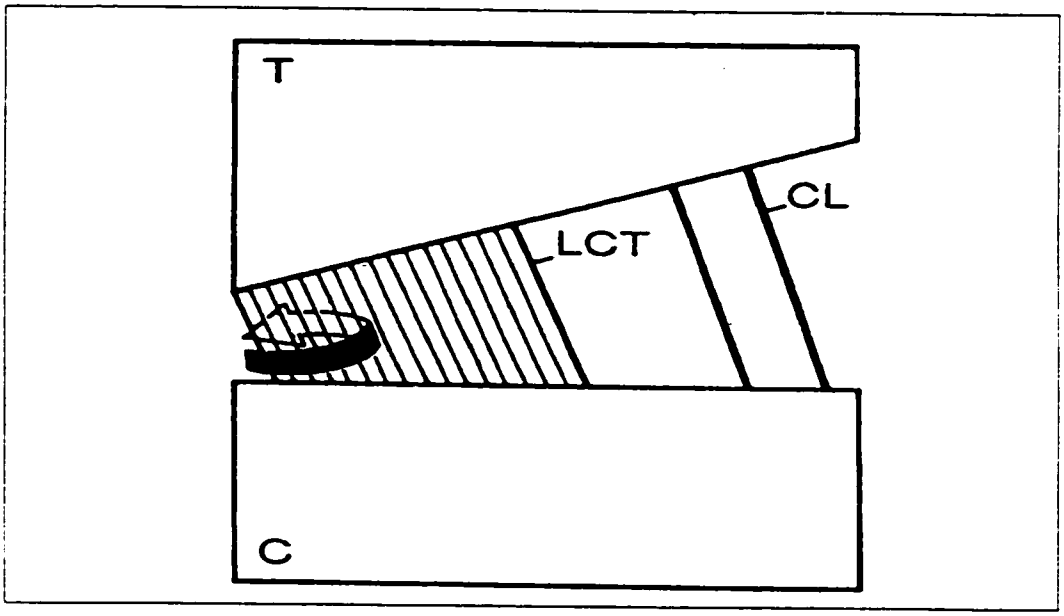

Figure 2. The talocalceneal ligament (LCT) and the cervical ligament (CL) in the talocalceneal joint (Stiehl, 1991).

Function

The subtalar joint axis is described as an oblique axis. It takes a postero-anterior direction from the postero-latero-inferior heel and exits the foot medio-superiorly. It deviates 41^0 from the horizontal plane and 17^0 from a sagittal plane that passes in

between the first and second toes (Murphy, 1993). Movement around the subtalar joint axis takes place in three planes, the frontal, transverse, and the sagittal plane. Motions in the frontal plane are eversion and inversion of the foot. Eversion is the motion where the lateral aspect of the foot is elevated. Inversion is the elevation of the medial aspect of the foot. In the transverse plane there are minimal abduction-adduction motions around the joint axis. Abduction is the rotation of the foot outward and adduction is the rotation of the foot inward. The motions in the sagittal plane are constituted of dorsiflexion and plantar flexion.

The motions in the three planes occur simultaneously during movements of the subtalar joint. The resultant triplanar motions are called pronation and supination. Pronation includes eversion, abduction, and dorsiflexion. Supination consists of inversion, adduction, and plantar flexion (Rockar, 1995). The range of these motions has not been accurately determined, due to the difficulty of separating the motion at the subtalar joint from the motion at the ankle joint (Sangeorzan, 1991). Due to the complexity of the movements around the subtalar joint axis, some researchers suggested a helical motion (Murphy, 1993). A screw-like motion where the rotation of the talus on the calcaneus is coupled with anterior and posterior translation, just like a screw moves forward as it is turned.

The Transverse Tarsal Joint

Structure

The transverse tarsal joint (Chopart's joint) is the compound joint formed by the talonavicular and the calcaneocuboid joints. The talonavicular joint is formed by the

convex head of the talus and the concave posterior aspect of the navicular and it is associated with the talocalcaneonavicular joint (Moore, 1992). The joint is reinforced inferiorly by the plantar calcaneonavicular (spring) ligament, which supports the head of the talus, the deltoid ligament medially, and the bifurcate ligament laterally. The capsule of the talonavicular joint is the same capsule that encloses the anterior and middle facets of the subtalar joint (Norkin & Levangie, 1992).

The calcaneocuboid joint is formed by the anterior end of the calcaneus and the posterior aspect of the cuboid. The articular surfaces of the two bones are saddle shaped making the motions at this joint more restricted than that of the talonavicular. The calcaneocuboid joint has its own articular capsule that is reinforced by the lateral band of the bifurcate ligament, the dorsal calcaneocuboid ligament, the plantar calcaneocuboid (short plantar) ligament, and the long plantar ligament (Norkin & Levangie, 1992).

Function

The talonavicular and calcaneocuboid joints together form an S shaped joint that traverses the foot and separates the hindfoot from the midfoot. The navicular and cuboid bones are essentially immobile bones, therefore, the motion at the transverse tarsal joint is considered to be the motion of the talus and the calcaneus on an almost fixed naviculocuboid unit (Norkin & Levangie, 1992).

Movements at the transverse tarsal joint take place around two axes of rotation: the first is the longitudinal axis, which is inclined anterodorsally at an angle of 15° and pointed away from the midline of the foot in the anteromedial direction at an angle of 9°

(Zatsoirsky, 1998). Pronation and supination take place around this axis with the inversion/eversion components predominating (Norkin & Levangie, 1992). The second axis of the transverse tarsal joint is the oblique axis, which rises up about 52° anterodorsally and is directed at an angle of 57° from the midline of the foot. Movements around this axis consist of flexion and extension of the midfoot (Frankel & Nordin, 1980).

Flexion and extension of the midfoot has been explained in terms of two parallel axes in the frontal plane (Zatsoirsky, 1998). The first axis passes through the talar neck and the second through the calcaneal body. When the foot is in eversion, the two axes are parallel and the midfoot is able to flex and extend easily. However, when the foot is in inversion, the two axes cross each other in the same frontal plane resulting in flexion and extension of the midfoot being restricted (Frankel & Nordin, 1980).

Muscles Affecting the Ankle and the Subtalar joints

The foot muscles can be divided, based on their attachments, into intrinsic and extrinsic. The intrinsic muscles of the foot include two muscle on the dorsal aspect and four layers of muscles on the plantar aspect. The dorsal muscles are the extensor digitorum brevis and the extensor hallucis brevis. The former attaches to the lateral surface of the calcaneus, and to the proximal phalanx of the big toe and the lateral aspect of the extensor digitorum longus tendon of digits 2-4. The latter attaches to the dorsal aspect of the calcaneus and the to the distal phalanx of the big toe.

The superficial layer of the plantar muscles of the foot includes the abductor hallucis, the flexor digitorum brevis, and the abductor digiti minimi. All three muscles extend from the posterior aspect of the calcaneus to the phalanges (Moore, 1992). The second layer consists of the quadratus plantae and the lumbricals. The quadratus plantae attaches to the calcaneus and the tendon of the flexor digitorum longus. The four lumbricals attach to the tendon of the flexor digitorum longus and the proximal phalanges. This layer also includes the tendon of the flexor hallucis longus, which attaches to the distal phalanx of the big toe.

The third layer of the plantar muscles of the foot includes the flexor hallucis brevis, the adductor hallucis, and the flexor digiti minimi. The flexor hallucis brevis attaches to the plantar surface of the cuboid and the first phalanx. The adductor hallucis attaches to the bases of the second, third, and fourth metatarsals and the base of the first phalanx of the hallux.

The fourth layer consists of the three plantar and four dorsal interossei muscles. Each dorsal interosseus attaches to the adjacent side of the neighbouring metatarsal bones and to the base of the first phalanges of 2^{nd} to 4^{th} digits. The plantar interossei attach to the bases of the third, fourth, and fifth metatarsals and to the first phalanges of 3^{rd} to 5^{th} digits (Rockar, 1995).

According to some writers, the action of the intrinsic muscles of the foot as a group is not fully understood (Rockar, 1995). However, other writers assign, to the muscle groups in the sole of the foot, the function of enabling the person to stand on uneven ground through a combination of movements such as flexion, abduction, and adduction of the digits. They also help maintain the arches of the foot (Moore, 1992).

The extrinsic muscles of the foot act on the foot-ankle complex including the subtalar joint. They can be divided into three groups; the anterior, the lateral, and the posterior group. The anterior group includes the extensor digitorum longus, the peroneus tertius, the extensor hallucis longus, and the tibialis anterior. The proximal attachment of this group is on the tibia or fibula. They attach distally on the dorsal aspect of the foot including the tarsals, metatarsals, and the phalanges except tibialis anterior, which inserts on the medial and inferior aspects of the medial cuneiform and the base of 1st metatarsal. Therefore, this group functions mainly as dorsiflexors, and the case of tibialis anterior also invertor, of the foot and extensors of the toes (Moore, 1992).

The lateral group of the extrinsic muscles of the foot include the peroneus longus and the peroneus brevis. Longus attaches distally on the plantar aspects of the base of 1st metatarsal and medial cuneiform. Brevis attaches on the dorsal aspect of the 5th metatarsal. Therefore, they evert the foot. They also plantar flex it because their tendons pass posterior to the lateral malleolus.

The posterior group of extrinsic foot muscles is divided into two layers; superficial and deep. The superficial layer includes the gastrocnemius, soleus, and plantaris muscles. All three muscles attach distally on the posterior aspect of the calcaneus through the Achilles tendon. Hence, they serve to lift the heel and plantarflex the foot. The deep layer of the posterior muscle group consists of the flexor hallucis longus, the flexor digitorum longus, and the tibialis posterior. They attach on the plantar surface of the foot, and their tendons pass deep to the flexor retinaculum of the ankle. These muscles serve to stabilise the leg on the foot during standing and to plantarflex the foot (Moore, 1992).

Skating Kinematics

The ice skating movement, like other human locomotion patterns, is biphasic. Each stride of forward skating consists of a period of double support followed by a period of single support (Humble & Gastwirth, 1988). The skating cycle consists of the push-off phase (encompasses wind up, release, and follow-through) and the recovery phase. The ankle angle is in dorsiflexion during wind up, neutral during release, plantar flexion during follow-through, and dorsiflexion during recovery (Minkoff, Varlotta, and Simonson, 1994). During the push off section of a stride, due to low friction between skate blade and ice, the skate is positioned at an angle away from the direction of movement. This angle is called the angle of propulsion, and is produced by externally rotating the leg at the hip. The positioning of the skate on an angle provides for better friction between the blade and the ice (Humble & Gastwirth, 1988). It is suggested that maximum thrust could be achieved when the angle of propulsion is 45°(Minkoff,

Varlotta, and Simonson, 1994).

The first three strides are the most important in forward skating, because the greatest period of acceleration begins after the first movement from a stationary position and lasts for about 1.25 seconds (Marino, 1976). During those strides the skater rotates the leg externally and begins the drive forward immediately upon touchdown. The first three strides are usually short and quick with the weight concentrated on the medial sides of the blades to increase friction (Humble & Gastwirth, 1988).

During forward acceleration, between touch down and heel off in the contact phase, the ankle joint goes through dorsiflexion and pronation. Plantar flexion and supination immediately follow this position. During this phase, the angle of propulsion and the forward lean are greatly increased allowing the ice reaction force to produce forward impulse that results mainly from plantar flexion as the skater pushes the toe of the skate against the ice. However, the support that exists around the ankle in skates limits plantar flexion of the ankle by restricting the range of motion (Hoshizaki, Kirchner, and Hall, 1989). The push-off phase (wind-up, release, and follow through) suffers from the lack of the powerful plantar flexion developed by the triceps surae and the reduction in muscular control of the ankle negatively affects speed and manoeuvrability (Minkoff, Varlotta, and Simonson, 1994). The position of the foot inside the skate and the ankle support that exist around the ankle have indications in terms of foot pain: For example, abnormal pronation at the subtalar joint produces pain in skates sooner than in everyday footwear because the rigid upper aspect of the skate causes severe pressure on the medial

side of the foot and the lateral side of the shank (Humble & Gastwirth, 1988).

Three Dimensional Reconstruction

The principle of 3-D reconstruction is to change two-dimensional co-ordinates taken on at least two images (two photographs or two films) into three-dimensional co-ordinates (Murphy, 1988). The filming process is, basically, the mapping of object (O) to image (I') in the film plane (Figure 3a). This image is projected again to image (I) in the projection plane (Figure 3b). Three-dimensional reconstruction is the process through which object (O) can be directly related to image (I) (Kwon, 1999).

One of the most commonly used 3-D reconstruction techniques is the Direct Linear Transformation (referred to as DLT). This technique, which was developed by Abdel-Azziz and Karara (1971), consists of the following algorithm:

$$x \pm \Delta x = \frac{L1X + L2Y + L3Z + L4}{L9X + L10Y + L11Z + 1}$$

$$y \pm \Delta y = \frac{L5X + L6Y + L7Z + L8}{L9X + L10Y + L11Z + 1}$$

where: x and y are the 2-D co-ordinates of a point.

$\Delta x, \Delta y$ are random errors resulting during the digitising process.

X, Y, Z are the 3-D co-ordinates of a point

L1 to L11 are the DLT parameters (they define the position and orientation of the camera)

The DLT parameters are determined through a calibration process using known 3-D points. Those parameters are entered into the algorithm with the 2-D co-ordinates of

points on the experimental object. Then, the 3-D co-ordinates of these points are obtained (Murphy, 1988).

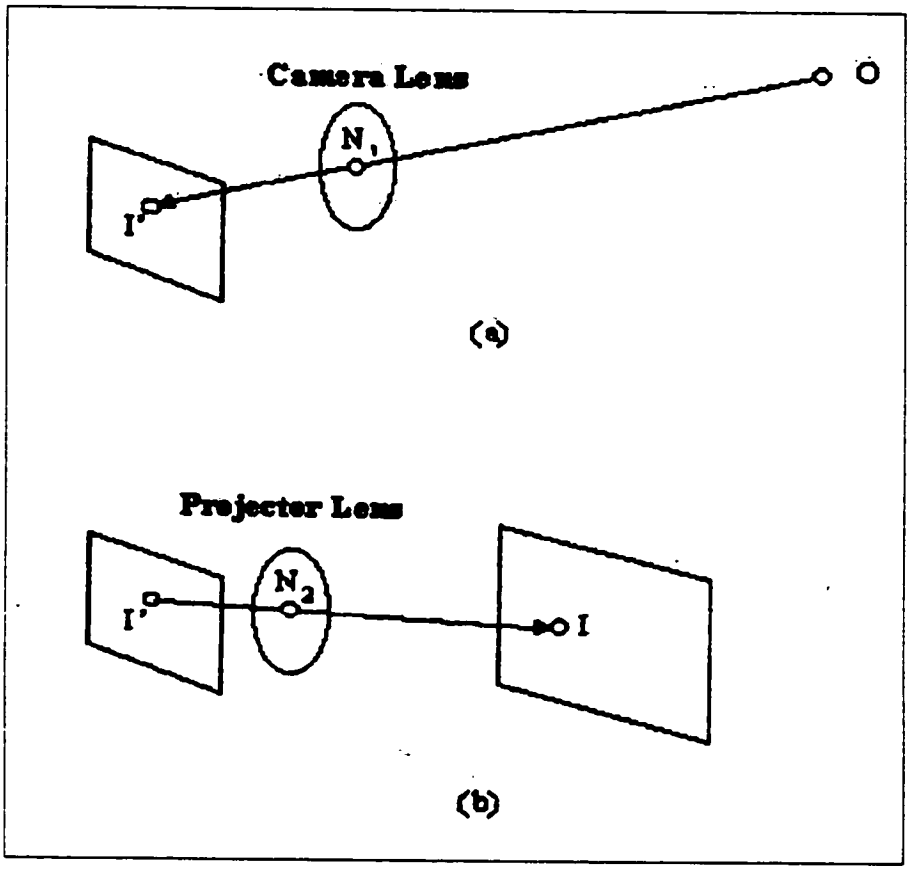

Figure 3. The principle of 3D reconstruction (Kwon, 1999)

Locating points in space using the DLT method was shown to provide adequate accuracy for human movement research (Shapiro, 1978). The greater mathematical complexity of DLT, compared to other methods, allows for a simple filming procedure (Dapena, Harman, and Miller, 1982). However, to preserve and improve the accuracy of DLT, certain conditions should be considered. These include factors such as the distribution and number of the control points. The best results are often obtained when the control points are distributed uniformly across the calibrated space. Configurations

that allow disproportionate concentration of control points in one area of the calibrated space would not produce accurate results (Chen, Armstrong, and Raftopoulos, 1994).

The number of control points is also important for the accuracy of DLT. In theory, six control points are enough to supply the 11 DLT parameters. However, increasing the number of control points allows for a more even distribution in the calibrated space. It also increases the redundancy of the system so the influence of individual random errors of the points is reduced. Additional control points also reduce the influence of systematic errors (Chen, Armstrong, and Raftopoulos, 1994).

The DLT method has been used in several studies that examined the difference between motions based on skin or shoe markers and motions based on bone markers. One such study found that markers mounted on the shoe overestimate motions at the ankle/subtalar joints (plantar/dorsiflexion, in/eversion). The overestimation exceeded 100% in some cases (Reinschmidt, Bogert, Lundberg & Nigg, 1997).

Studies that examined the bone motion underlying the skin and footwear motions have mostly relied on inserting metallic markers in the bone for stereoradiography (Lundberg, 1989) or markers attached to intracortical bone pins for stereovideography (La fortune et al., 1994; Reinschmidt et al., 1997). Both these methods come at the expense of great discomfort and invasiveness to the subject. Determining identical bony landmarks on two radiographs without using invasive procedures has been achieved in studies of some spine disorders such as scoliosis (Pearcy, 1985). This method relies on

finding anatomical features on the bone that can be invariant on both images such as the centre of vertebral endplates. It could also be used for structures like the head of the femur where the centre of its circular image on a radiograph can be identical in two views (Allard, Stokes, and Blanchi, 1995). However, to the knowledge of this author, this method has not been used in stereoradigraphic studies of the foot.

Summary

The predominant motions at the ankle and subtalar joints are plantar/dorsiflexion and in/eversion respectively. Hockey skating is a bi-phasic motion, where a period of double support is followed by a period of single support. The first three strides in forward acceleration resemble running on skates and they are the most important because, the greatest period of acceleration takes place during these strides. Between touchdown and heel-off the ankle goes through dorsiflexion and pronation followed by plantar flexion and supination. However, these motions are restricted due to the rigid support around the ankle, which results in a limited range of motion. Very few studies examined the difference between the motion of footwear and the actual motion of the bony segment. Nevertheless, the ones that did concluded that footwear motion overestimates the actual motion. This overestimation could reach up to a 100% in some cases.

MATERIALS AND METHODS

Subjects

Eight healthy male university students of ages between 20 and 24 years participated in the study. All subjects had size 9 feet and were skilled skaters with no morphological deformations or anomalies of the lower leg or feet. Participants signed an informed consent form that explained the experimental procedure and the study was approved by the University of Ottawa Research Ethics Board.

Instruments

X-ray Calibration Cage

A 50x50x50 cm Plexiglas calibration cage was constructed for the x-ray measurements. The cage included a movable platform for the foot while in the skate. The platform rested on a 20cm-high fulcrum, made of Plexiglas and fixed at mid point of the floor of the cage, which allowed it to move freely. The platform also had a hole in the front and a hole in the back for two Plexiglas bars that extended to the sides of the cage. Those two bars went through holes made in the side of the cage at positions that corresponded to 15° of dorsiflexion, neutral position, and 28° of plantar flexion with 45° of external rotation. The magnitudes of dorsiflexion and plantar flexion are based on skate stiffness data (Hanckok, 1999). The superior aspect of the cage consisted of two mobile sheets of Plexiglas with each having a half circular area cut off and padded to fit tightly around the shank of the subject and prevent its movement (Figure 4). Eighty-five lead spheres of 2mm diameter were embedded in the front and back sides of the

calibration cage (34 in the front and 51 in the back). The spheres were distributed such as to cover as much of the areas of the sides as possible (Figure 5). The number of spheres was reached at through adding spheres to the sides of the calibration cage until it was deemed sufficient to cover enough of the area as to have a minimum of six markers on each side in every x-ray image. Six is the minimal number of control points needed for the Direct Linear Transformation algorithm to work. However, a large number of control points allows for an even distribution through the calibrated area and reduces error (Chen, Armstrong, and Raftopoulos, 1994). There is no danger of the lead spheres masking other data because of their small size. In addition, the lead spheres used as skin and skate markers are larger than the ones used as control points (5mm Vs 2mm). The three dimensional coordinates of the spheres were measured in relation to an origin in the right front-lower corner of the cage, where the X-axis was parallel to the front side of the cage and positive from right to left. The positive direction of the X-axis (from right to left) was necessary because the location of the origin at the front right corner of the cage was imposed by the shape and functionality of the digitizing arm used to measure 3D coordinates. However, the positive direction of the X- axis has no bearing on the data because it will be corrected by the software used to reconstruct the 3D coordinates. The Y-axis was parallel to and positive in the direction of the depth of the cage. The Z-axis was vertical and positive in the downward direction. The measurement of the 3D coordinates was made using a three dimensional digitising arm (Microscribe model 3D, Immersion Co., USA) with a manufacturer-determined error of 0.3 mm that was also validated in the laboratory in an unpublished work by this author. The lead spheres with

known 3D coordinates were used as control points for the three-dimensional reconstruction.

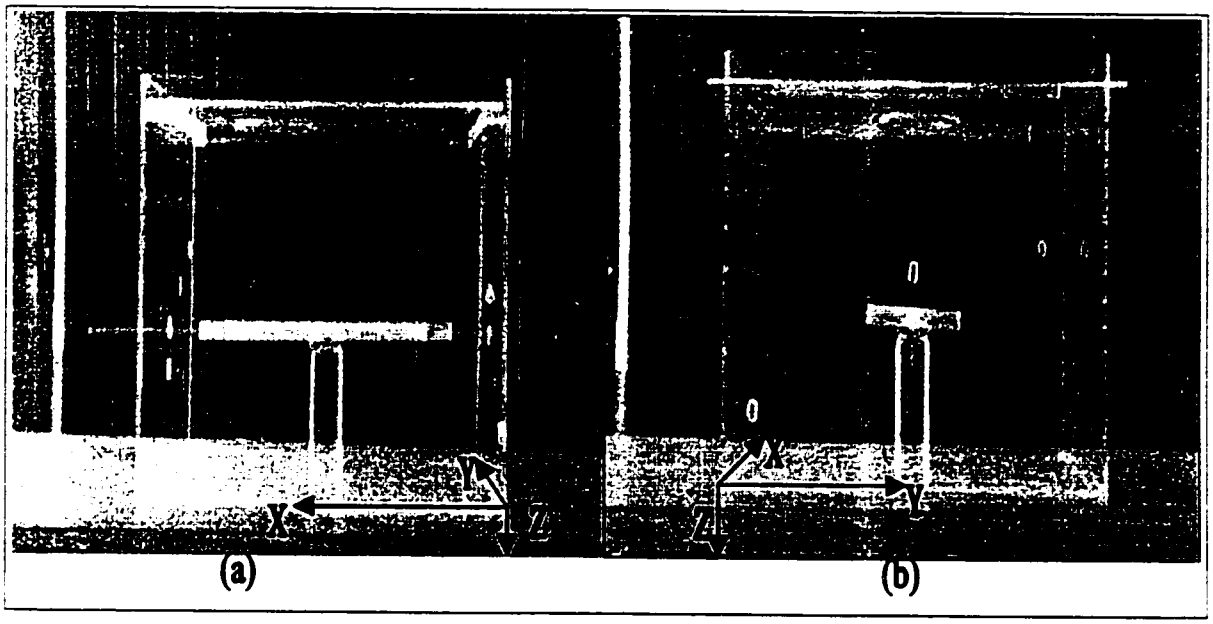

Figure 4. The x-ray calibration cage; a frontal view facing the x-ray source (a) and a side view (b).

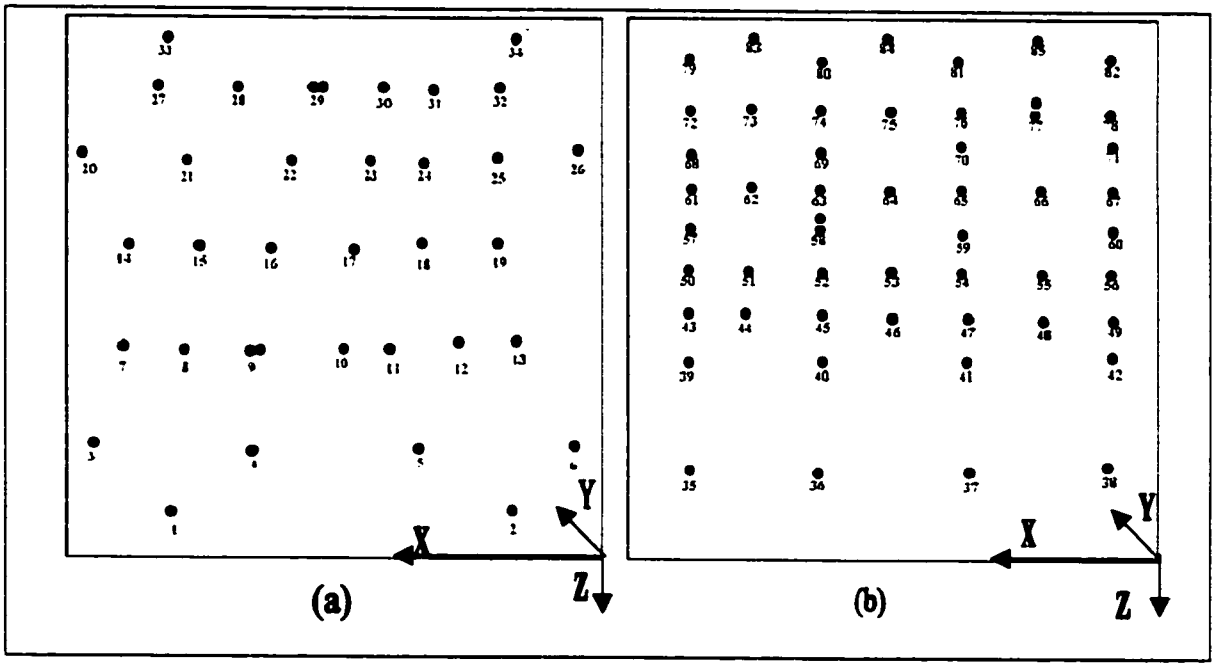

Figure 5. Distribution of control points (lead spheres) in the sides of the calibration cage, front (a) and back (b).

Altered Skate

As can be seen in figure 6, three openings of 2cm diameter were made in a right hockey skate in the area above the tarsus of the foot. The first hole was made 3cm above the outer sole of the skate and 4cm from the heel cup, the second was 1cm directly above the first, and the third hole was made to the left of the other two at 2cm from both. This meant that the closest two skin markers to each other (Skin1 and Skin2) are 3cm apart (the radius of each hole is 1 cm and the distance between the two holes is 1 cm) which is enough to prevent confusion in digitizing. After examining the structure of a cut up skate and in consultation with a mechanical engineer, the holes were placed so that they did not disrupt any supporting parts in the body of the skate. This ensured that the integrity of the skate structure was preserved. The locations of the skin markers above the lateral aspect of the tarsus were based on the convention commonly used in kinematic studies; where a triad of markers that represent the foot as a rigid segment is placed behind the line of the tarsometatarsal joints (Reinschmidt, 1997). Three 5mm lead spheres were covered with reflective tape and attached to the body of the skate in non-coplanar locations. These markers represented the motion of the skate boot. Another three markers were fixed on top of plastic screws to serve as skin markers that will protrude through the openings in the skate. The skate was "broken in" through several hours of skating before the testing procedure.

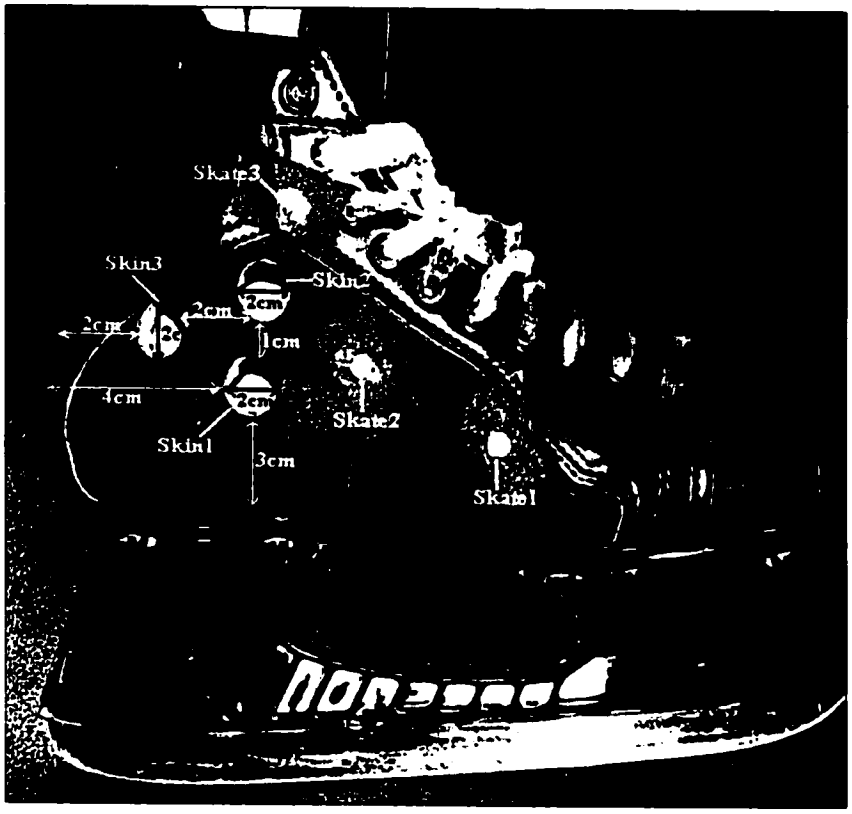

Figure 6. Altered skate, showing skin and skate markers locations.

Video Cameras

Filming on the ice was performed using two high-speed video cameras (200 Hz, JC Labs, California, USA) mounted on a mobile platform, which rolled on rail sections (4 x 2m x 0.65m) built out of halved PVC piping. The cameras tracked the subject on line parallel to his line of motion. (Lafontaine, 2000)

Ariel Performance Analysis System (APAS)

Software developed by Ariel Dynamics, which was used to capture the video films to the computer. The same software was used to digitize markers and obtain their 3D coordinates through the implementation of the DLT algorithm, which allowed the reconstruction of the three-dimensional motion. However, it was not possible to use

APAS to digitize x-ray images because they were not *.AVI files. Therefore, some modifications had to be made to enable the software to deal with still images; the x-ray images were scanned as *.PCX files. Each PCX file was duplicated five times (the minimum number of film sequences required by APAS) and stored in a directory that has the same name. For example, the dorsiflexion images were stored in the C: directory as follows:

C:\DFB\DFB1.PCX
C:\DFB\DFB2.PCX
C:\DFB\DFB3.PCX
C:\DFB\DFB4.PCX
C:\DFB\DFB5.PCX

In the same directory as above a *.PCL file was stored. This file was a text file that had the same name as the PCX files and was used to tell the software the order of the PCX images. It contained the following information:

c:\DFB\DFB1.PCX
c:\DFB\DFB2.PCX
c:\DFB\DFB3.PCX
c:\DFB\DFB4.PCX
c:\DFB\DFB5.PCX

In essence, the steps mentioned above were designed to mimic a film sequence to enable the software to read the x-ray files.

Procedures

Marker placement

A thin 1mm piece of thermoplastic (Thermoform) was heated and molded in the shape of the skin area directly above the lateral aspect of the tarsus of the foot of each subject (Figure 7). Medical adhesive was used to attach the thermoplastic to the skin and

the three plastic screws, with the lead markers fixed on their tops, were glued to the thermoplastic after the subject put on the skate. The three markers representing the skin motion protruded through the openings that were made in the skate.

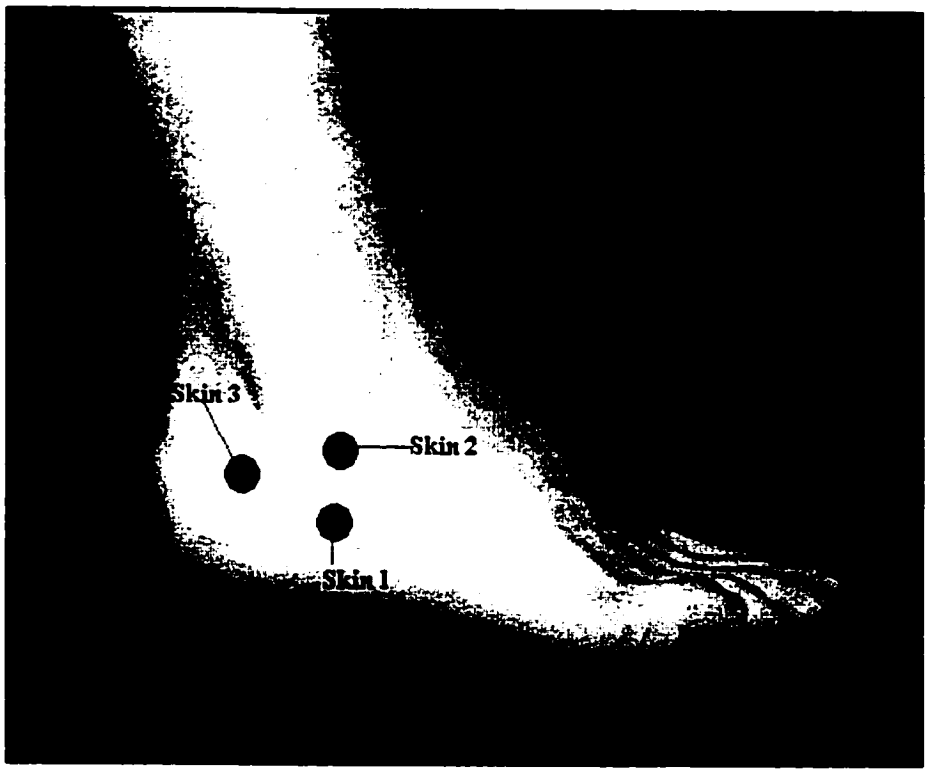

Figure 7. The positions of the Thermoplastic and skin markers on the foot

X-ray and video capture

The subject dressed in a black skin-tight outfit was wearing the modified skate with the boot and skin markers on his right foot, and the skate was placed in a slot made in the Plexiglas platform (Figure 8a). The slot was lined with a rubbery material and the skate fit into it snugly, preventing any rocking movements. An x-ray source was placed facing the right lateral side of the subject's foot and the x-ray film was attached to the opposite side of the Plexiglas box. Two films were exposed for each of three positions of the foot; full dorsiflexion, neutral, full plantar flexion with 45° of external rotation (Figure

8b). The angles were chosen to simulate a push off phase in forward skating motion. The x-ray source was placed in a horizontal position, 0° in relation to the platform, for the first exposure. The second exposure was at a 30° angle with the first one (Figure 9).

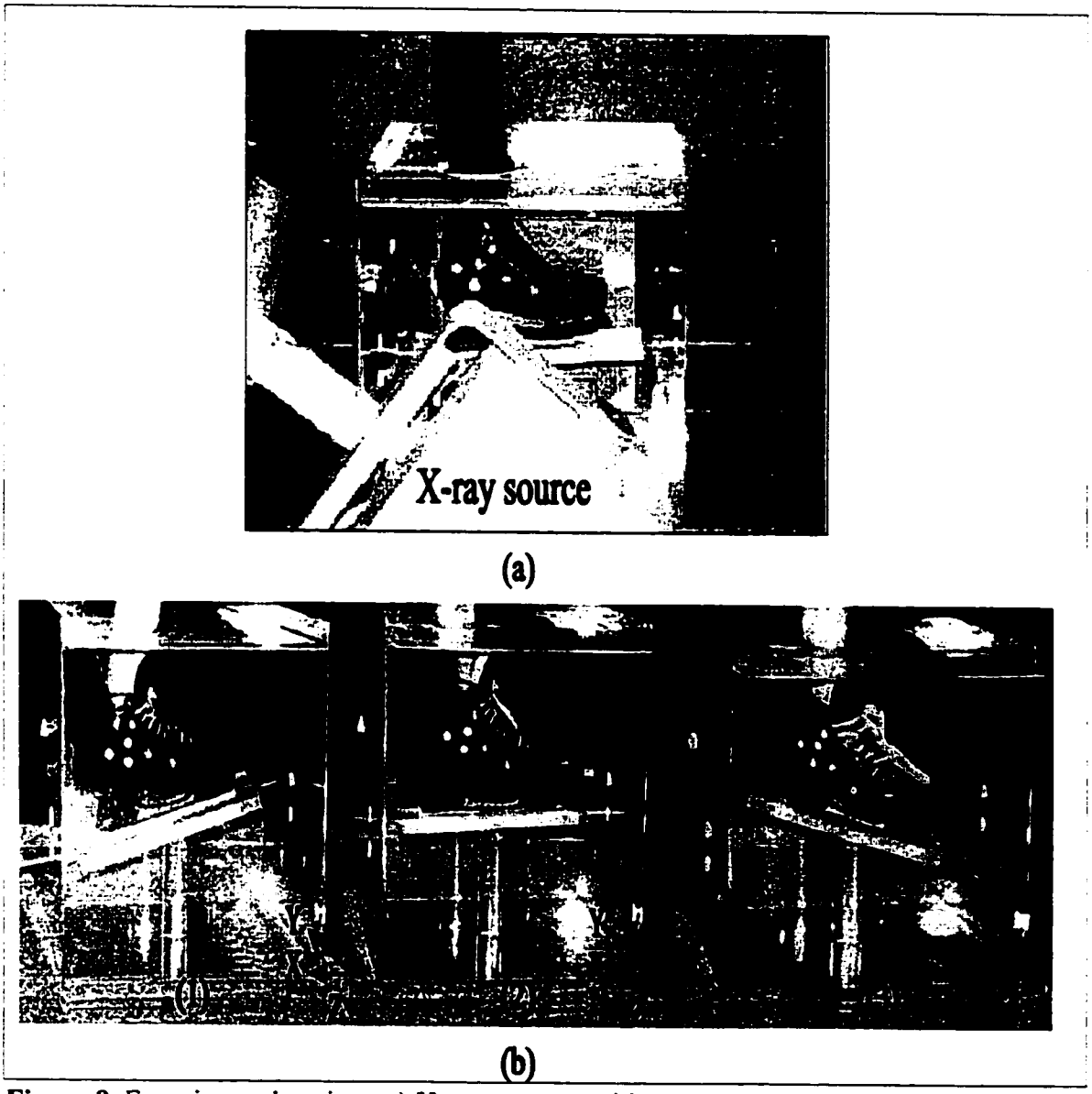

Figure 8. Experimental setting: a) X-ray source position

b) Foot positions; dorsiflexion (1), neutral (2), dorsiflexion (3).

The choice of a 30° angle was made because it allows both x-ray images to show the lateral aspect of the tarsal bones, which makes the identification of the same bony landmarks on the two images possible. This was determined after running a pilot test of the procedure in the laboratory. The x-ray procedure was conducted in the presence of a radiology technician in the change room of the arena.

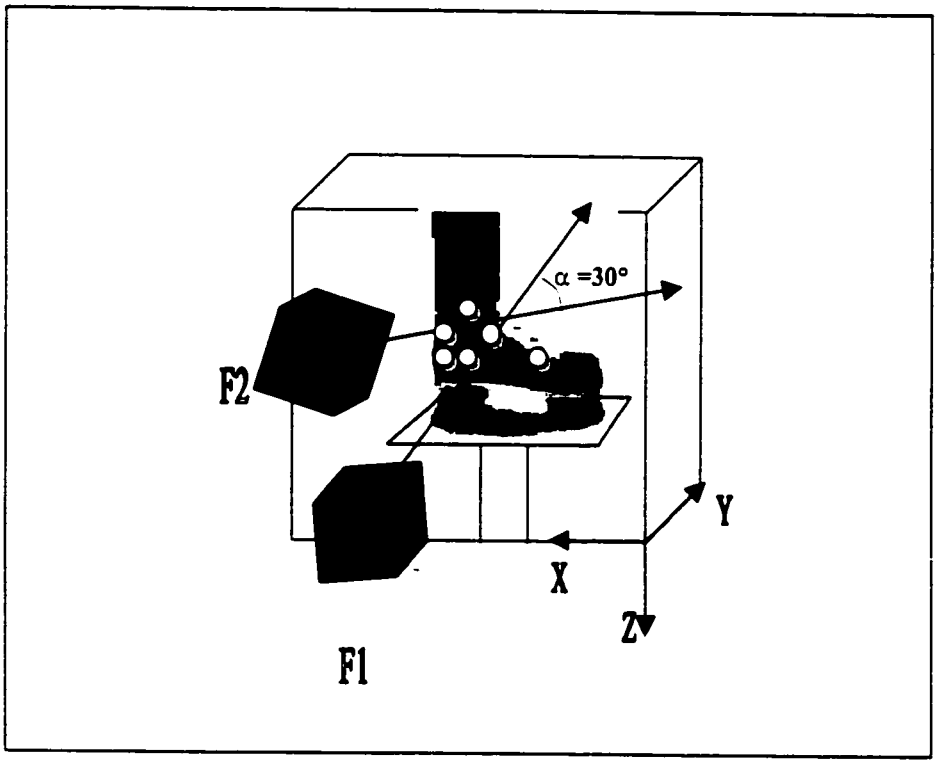

Figure 9. Experimental setting: positioning of the x-ray source: F1 at horizontal position and F2 at 30° with F1.

After the x-ray session the subject headed directly to the ice, where the video capture took place. The subject was told to warm up by skating around the rink for about 3 minutes, then he performed four trial runs of the actual skating motion. The ice session started with filming a calibration frame that supported 16 reflective markers (Figure 10) whose 3D coordinates were measured by the 3D digitizer (Microscribe 3D). The 3D

coordinates of the control points on the calibration frame were the average of 10 measurements. After calibration, the subject performed 10 trials of forward skating and was filmed by the two high-speed video cameras that tracked his motion along the first three strides, including the start, at a rate of 200 Hz. The first three strides were filmed because they are the most dynamic part of a skating motion and the greatest period of acceleration takes place during those strides (Marino, 1976).

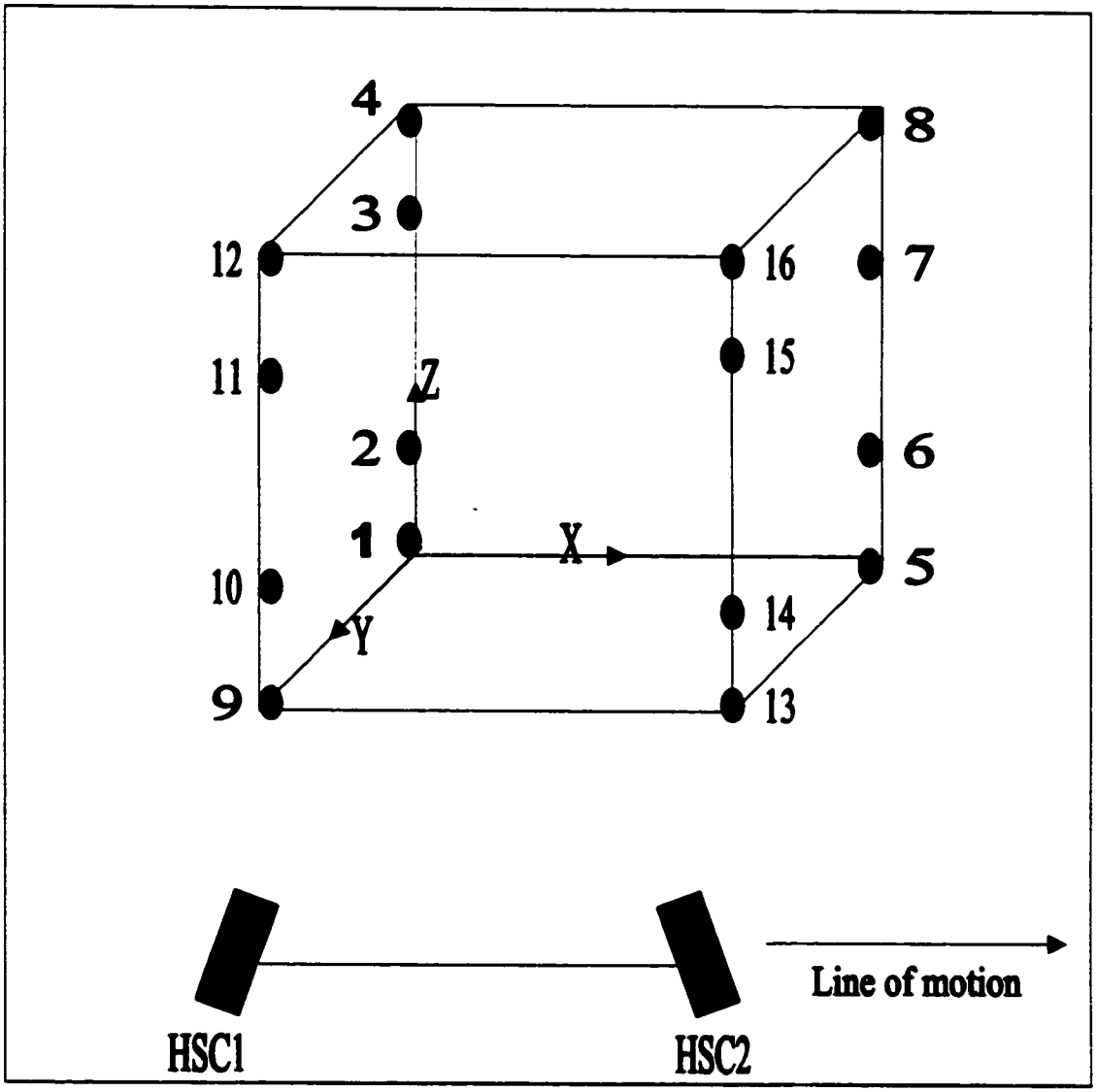

Figure 10. Experimental setting on the ice: calibration frame and the two high-speed cameras (HSC1 and HSC2).

Data processing

Two x-ray images for each of the foot positions (dorsiflexion, neutral, plantar flexion) were scanned into the computer as PCX files using a Scanjet ADF scanner. Markers representing bone, skin and skate were digitised on the two views of each position using APAS. The centres of spherical bony structures of the head of the talus, the body of the talus, and the cuboid bone were selected as invariant points on both images and were used to represent the motion of the bone (Allard, Stokes, Blanchi, 1995). These centres were determined visually in relation to the edges of each bony structure. The three dimensional coordinates of bone, skin, and skate markers were obtained for each of the foot positions using the DLT algorithm incorporated in the transformation procedure in APAS. The use of one x-ray source that was moved from one position to the second should not negatively affect the calculation of 3D data. The subject, with his shank anchored, was told to stay still for the few seconds it took to rotate the x-ray source 30° upwards, which was not difficult since the subject's foot is well fixed within the x-ray cage limiting its movement. This procedure is used when finances do not allow for two X-ray sources (Andre et al, 1994; Berthonnaud et al, 1998).

Typically in kinematic studies, three markers on a body segment are used to represent its motion. Therefore, it is useful to know the position and path of the centroid of those three markers to describe the motion of the segment they represent. Hence, the spatial position of the centroid of every set of three markers (bone, skin, skate) was calculated at dorsiflexion, neutral position, and plantar flexion (see appendix A). Then the spatial distances between the centroids (bone-skin, skin-skate, skate-bone) were

calculated at those positions in order to describe the three motions in relation to each other.

Considering that the centroids only describe the segment motion and do not indicate the magnitude of the difference amongst the motions of each type of marker, the rotations of the foot from dorsiflexion to plantar flexion through the neutral position needed to be obtained from each type of marker. Using vector cross product (see appendix B), the rotations of a vector that passes through two bone markers, a vector that passes through two skin markers, and a vector that passes through two skate markers (Figure 11) were calculated. The centres of the head and body of the talus were chosen to define the bone vector and markers 2 and 3 from both skin and skate to define skin and skate vectors. Bearing in mind that regardless of which pair of markers used to define a vector, the result should be the same. Hence, in order to compare foot rotations based on the different types of markers, vector rotations from the neutral position to dorsiflexion and from neutral position to plantar flexion were calculated. Note that the above mentioned vectors will be named bone, skin, and skate vectors for the remainder of this document.

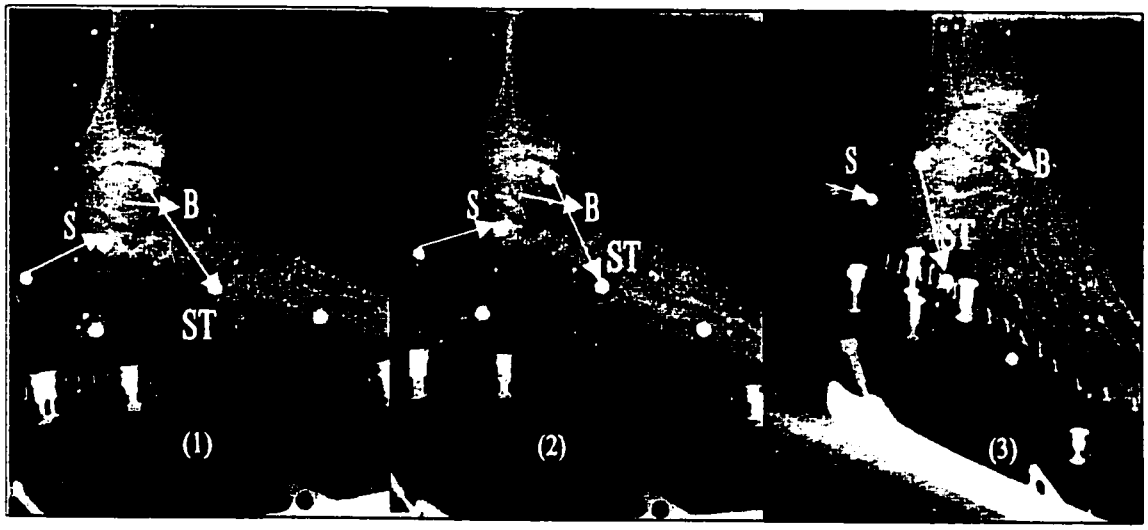

Figure 11. Foot rotation angles based on bone (B), skin (S), and Skate (ST) markers at dorsiflexion (1), neutral position (2), and plantarflexion (3).

The second stride of the skating motion was captured into APAS from each camera view of the trials on ice. Using the trim function in the same software, the push-off motion was determined from heel-off to toe-off and it encompassed ten frames for all subjects. Heel-off was defined as the moment the back end of the skate left the ice surface, and the toe-off was the moment the front end of the skate blade left the ice surface. Skin and skate markers were digitised on each of the frames, and the three-dimensional coordinates of the centroid of each marker type were calculated. The distance between the two centroids (skin, skate) was also determined at each frame of motion. The rotations of the foot from heel-off to toe-off were determined by using vector cross product to calculate the rotations of a vector that passes through two skin markers and a vector that passes through two skate markers from heel-off to toe-off.

Statistics

For the x-ray data, inter-centroid distances were calculated from two x-ray images for each subject at dorsiflexion, neutral position, and plantar flexion. These distances

were then averaged for all subjects. In order to determine which of the inter-centroid distances varied more than the other, the Coefficients of Variation (CV= [(STD/|Mean|) x 100]) were calculated for bone-skin, skin-skate, and skate-bone distances. The Coefficients of Variation was used because it allows for comparison of variability of different sets of observations. In order to find out which two centroids match each other's motion best, a paired samples t-test was utilized to determine whether the change in one inter-centroid distance was significant in relation to each of the other two distances (significance level at $p < 0.05$). The correlation between the inter-centroid distances was determined using the Pearson correlation coefficient (r). The rotations of the foot based on the different types of markers were calculated for each subject at each of the three foot positions then averaged for all subjects. A paired samples t-test and the Pearson correlation coefficient were used to compare the rotations of the foot to each other.

For the on-ice data, the inter-centroid distance of skin and skate markers was calculated at each frame of the push-off motion then averaged across three trials for each subject. The Coefficient of Variation (CV) was calculated across all frames. Foot rotations based on skin and skate markers were determined at heel-off and toe-off and an average of three trials was calculated for each subject. Skin and skate based rotations were compared using the paired samples t-test ($p<0.05$) and the Pearson correlation coefficient.

Accuracy measurements

Standard deviation was used as a representation of the range of error in three-dimensional reconstruction of the calibrated space: The distances between measured

(Microscribe) and digitized (APAS) values for ten markers on the calibration box were calculated using Root Mean Square, and considering that, in the case of no error, all these distances should equal 0, the range of error was represented by the standard deviation from the mean distance.

In order to determine the error (including systematic error) in digitizing markers on segments within the calibrated space, a skeleton foot that had metal wires inserted in it was x-rayed (Figure 12). The ends of the wires provided points that are invariant in two images. Therefore, six of the wire end-points were digitized five times each, and the distance between first and second, second and third, third and fourth, forth and fifth, and fifth and first measurements were determined and the standard deviation of those distances was calculated in order to establish the range of error in digitizing.

Determining identical bony landmarks on two x-ray images is a source of error due to the difficulty in finding two invariant points on separate radiographs. This difficulty stems from the fact that the x-ray image is the impression of different bone densities of the segment on the film. This study implemented the method of digitizing the centre of spherical structures on both radiographs (Allard, Stokes, Blanchi, 1995). However, this process has not been used on bony structures of the foot (tarsal bones) before. Therefore, the error in reconstructing three-dimensional coordinates of chosen bony landmarks was determined through repeatedly digitizing six bony landmarks on the skeleton foot (Figure 12). The following six bony landmarks were selected; the centre of the cuboid bone, the centre of the head of the talus, the centre of the body of the talus and three points on the

tibia. Each of these landmarks was digitized five times along with the previously mentioned six wire points on the same x-ray views. The distance between first and second, second and third, third and fourth, forth and fifth, and fifth and first measurements were determined and the standard deviation of those distances was calculated in order to establish the error in digitizing bony landmarks.

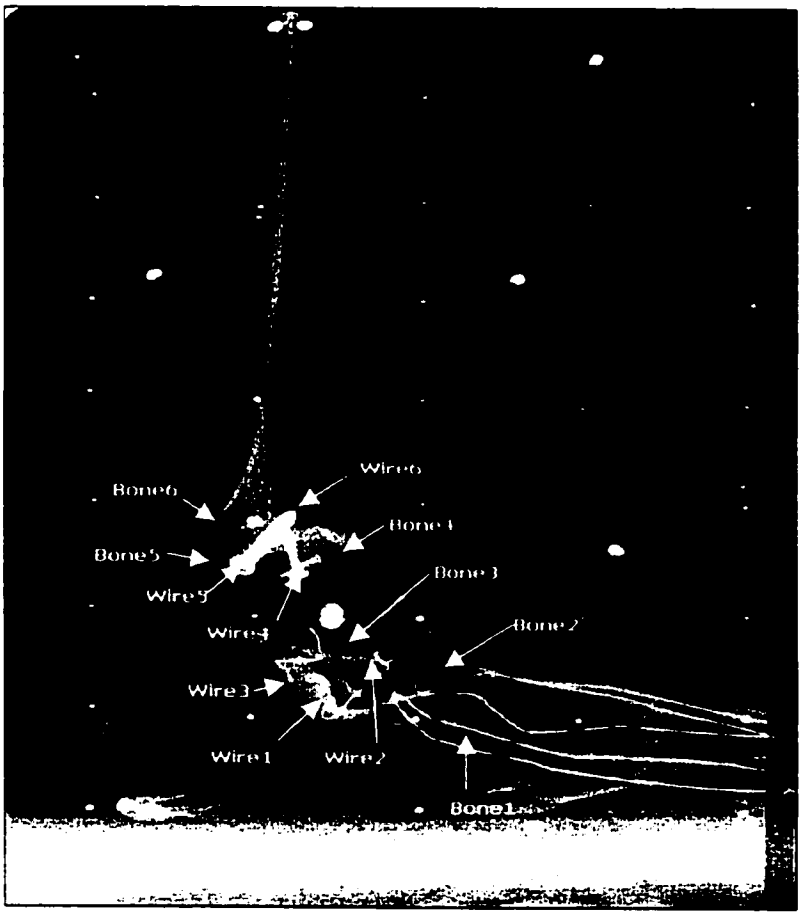

Figure 12. Wire points and bony landmarks used for error measurements.

Assumptions and limitations

Due to limited resources it was not possible to develop a computerized method by which skating kinematics that would discern foot motion in different planes (plantar/dorsiflexions, in/eversion, external/internal rotation) could be established. Therefore, vector angles were used to determine the differences between bone, skin, and skate motions during plantar/dorsiflexions, which was considered sufficient for the purposes of this study. The structure of the x-ray calibration box allowed for only limited loading of the examined foot. Considering that there is no standard loading value for a push-off motion, it was assumed that the amount of loading a subject could exert without breaking the platform is enough to mimic a realistic skating condition, because the subject is applying force on the platform and does not have to "carry" his foot. The x-ray part of the experiment was also limited by the fact that due to dosage amounts it was not possible to perform more than one trial per subject. Therefore, the results are based on the average of all subjects with no inter-subject comparisons. Furthermore, considering that it was not possible to use two x-ray sources, one x-ray source had to be moved between two positions indicating the assumption that the subject's foot does not move while the x-ray source is repositioned.

RESULTS

Inclusion of subject data

Problems were encountered with having sufficient number of common control points on the x-ray views, especially on the front side of the calibration box. Some subjects' results had to be dropped due to large errors in 3D reconstruction of markers. Therefore, the results used are for subjects 2,4,5,7, and 8. As for the ice data, some subjects' results had to be dropped due to marker merger and shadowing problems that could have been eliminated by using smaller video view. The results used for the ice session are from subjects 1, 5, and 6 for the centroids and 1,2,4.5, and 6 for the angles. For the centroid data on ice; Subjects 2, 3, 4, 7, and 8 had very few usable frames between heel-off and toe-off and had to be dropped because all ten frames of the motion were needed. In addition, subject 1 had only two usable trials; therefore, in order to use the same number of trials for all subjects, only two trials were used from subjects 5 and 6. In the case of angle data, only the first and last frames were needed to calculate the angles at heel-off and toe-off. Subjects 2 and 4, which were not used for the centroid data, had clear first and last frames in three trials. This allowed the use of three trials from subjects 1,2,4,5, and 6 for the angle data.

Accuracy

The error in 3D reconstruction was determined for the x-ray calibration box by calculating the distances between measured (Microscribe) and digitized (APAS) values for ten markers on the calibration box. The results in Table 1 show that the average distance was about 0.18 cm with a standard deviation of 0.11 cm. The points used were

all from the back side of the calibration box due to the limited number of points on the front side, which were all needed to be used as control points.

Table 1. Error in three-dimensional reconstruction of control points.

	Digitized			Measured			
Markers	X (cm)	Y (cm)	Z (cm)	X (cm)	Y (cm)	Z (cm)	RMS (cm)
1	29.26	49.54	-28.40	29.26	49.42	-28.39	0.12
2	33.75	49.03	-28.41	33.76	49.40	-28.41	0.36
3	38.34	49.31	-28.61	38.28	49.39	-28.61	0.10
4	29.27	49.33	-31.65	29.25	49.42	-31.67	0.08
5	38.28	49.21	-31.66	38.26	49.43	-31.65	0.21
6	29.28	49.19	-34.94	29.26	49.43	-34.91	0.23
7	33.70	49.57	-34.69	33.67	49.43	-34.78	0.16
8	38.19	49.59	-34.96	38.20	49.62	-35.02	0.06
9	29.32	49.84	-38.24	29.27	49.45	-38.34	0.41
10	38.28	49.44	-38.25	38.25	49.40	-38.34	0.10
						Mean	0.18 (0.11)

As for the error in digitizing; results in Table 2 show that the largest standard deviation of the distance between repeated measurements of the same points was 0.32 cm.

Table 2. Error in three-dimensional reconstruction of markers within the calibrated space.

	Distance measurements (cm)					
Wire points	1^{st}-2^{nd}	2^{nd}-3^{rd}	3^{rd}-4^{th}	4^{th}-5^{th}	5^{th}-1^{st}	Mean
1	0.21	0.43	0.44	0.09	0.31	0.29 (0.14)
2	0.28	0.24	0.63	0.15	0.06	0.27 (0.21)
3	0.00	0.19	0.1	0.73	0.62	0.32 (0.32)
4	0.04	0.26	0.34	0.08	0.07	0.15 (0.13)
5	0.33	0.22	0.71	0.65	0.49	0.48 (0.20)
6	0.09	0.58	0.67	0.45	0.45	0.44 (0.22)

The accuracy in reconstructing bony landmarks was determined by calculating the distances between repeated measurements of the same bony landmarks. The standard

deviation values of the repeated measures are shown in table 3, where the largest value was equal to 0.59 cm.

Table 3. Error in three-dimensional reconstruction of bony landmarks.

	Distance measurements (cm)					
Bone points	1^{st}-2^{nd}	2^{nd}-3^{rd}	3^{rd}-4^{th}	4^{th}-5^{th}	5^{th}-1^{st}	Mean
1	0.29	0.83	0.40	0.43	1.25	0.64 (0.40)
2	0.95	0.24	0.15	1.57	0.95	0.77 (0.58)
3	0.47	1.30	0.31	0.23	1.49	0.76 (0.59)
4	0.25	0.79	0.12	0.40	0.31	0.37 (0.25)
5	1.02	0.71	1.09	0.33	0.85	0.80 (0.30)
6	0.29	1.25	0.89	0.09	0.14	0.53 (0.51)

The error in 3D reconstruction of video views of the motion on ice was evaluated by comparing the distance between two digitized markers on the skate to the distance between the same two markers that were physically measured. The largest difference between the two distances was equal to 5% of the real distance (Lafontaine, 2000).

X-ray data

Three-dimensional coordinates of the centroids of each triad of markers were calculated at each of the three foot positions (dorsiflexion, neutral, plantar flexion). The distances between the centroids were calculated and then averaged for all subjects. As Table 4 shows, the values of coefficients of variation were 13% for the distance between bone and skin centroids, 36% for the distance between skin and skate centroids, and 26% for the distance between bone and skate centroids.

Table 4. Average* distances (cm) between centroids of bone, skin, and skate markers.

	Bone-skin	(std)	Skin-skate	(std)	Skate-bone	(std)
Dorsiflexion	06.92	(01.03)	07.75	(01.49)	08.86	(01.70)
Neutral position	06.58	(01.14)	05.68	(01.65)	06.18	(01.23)
Plantar flexion	08.31	(00.92)	11.56	(02.89)	10.68	(01.96)
CV%	13.00		36.00		26.00	

* 3D coordinates of individual markers for all subjects can be seen in appendix C.

All inter-centroid distances (bone-skin, skin-skate, and skate-bone) changed in positive correlation with each other from dorsiflexion to neutral position to plantar flexion (Table 5). A paired samples t-test (Table 5) shows that the difference in the distance is not significant for any pair of the centroids ($p>0.05$). However, statistical power for the t-test in this case is weak due to the small sample size (3 observations). The graph in figure 13 shows that inter-centroid distances increased at dorsiflexion and plantar flexion in comparison to the neutral position.

Table 5. Paired samples t-test and correlation values for average distances (cm) between centroids of bone, skin, and skate markers.

	Bone-skin Vs Skin-skate (n = 3)	Skin-skate Vs Skate-bone (n = 3)	Skate-bone Vs Bone-skin (n = 3)
p	00.47	00.72	00.27
r	00.99	00.96	00.90

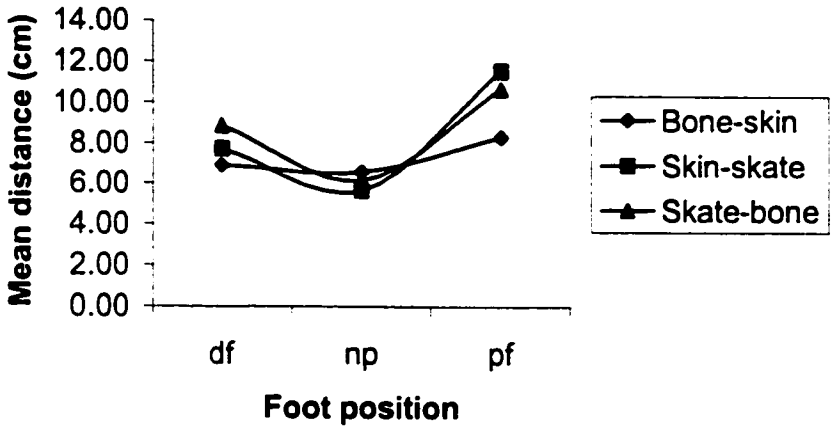

Figure 13. Average distances between bone, skin, and skate centroids at dorsiflexion (df), neutral position (np), and plantar flexion (pf).

Data in table 6 show the average coordinates of the centroids of bone, skin, and skate markers with the coefficients of variation as a measure of the variability of the coordinates across the three foot positions.

Table 6. Average 3D coordinates (cm) of bone, skin, and skate centroids at dorsiflexion (DF), neutral position (NP), and plantar flexion (PF) from x-ray data.

	Bone			Skin			Skate		
	X	Y	Z	X	Y	Z	X	Y	Z
DF	32.82	25.85	-30.88	36.19	20.16	-28.46	29.00	19.59	-27.94
NP	30.07	25.23	-32.09	33.02	19.52	-29.71	28.29	19.83	-29.01
PF	24.65	23.05	-34.59	33.43	21.58	-33.84	25.50	15.75	-26.04
CV%	14%	6.00%	5.00%	1.00%	7.00%	9.00%	7.00%	16%	7.00%

Data in table 7 show the rotations of the bone, skin, and skate vectors, which represent bone, skin, and skate motions, from dorsiflexion to neutral position and from neutral position to plantar flexion. During dorsiflexion the rotations show no specific trend with the mean rotations for all three types of vectors being almost equal. However, during plantar flexion skin rotations were the largest and skate rotations the smallest across all subjects. Mean skate rotation was 57% smaller than mean skin rotation and 27% smaller than mean bone rotation, while mean skin rotation was 42% larger than mean bone rotation. It is also clear that skate and bone rotations from neutral position to plantar flexion were systematic across all subjects (skate rotations about 70% of bone rotations) except for subject 2.

Table 7. Bone, skin, and skate vectors' rotations from dorsiflexion to neutral position and from neutral position to plantar flexion.

	Dorsiflexion to Neutral position (Deg)			Neutral position to plantar flexion (Deg)		
Subject	Bone	Skin	Skate	Bone	Skin	Skate
2	08.42	13.39	11.67	28.84	36.83	27.59
4	13.67	09.54	10.37	20.59	45.03	12.35
5	10.53	10.09	08.45	28.83	42.07	17.04
7	15.80	09.14	08.02	22.48	43.79	17.55
8	13.57	13.94	09.02	26.88	51.59	19.10
Mean	12.40	11.22	09.51	25.53	43.86	18.73
	(2.91)	(2.27)	(1.50)	(3.79)	(5.33)	(5.56)

For dorsiflexion, a paired samples t-test in table 8 showed no significant difference in vector rotations between bone and skin vectors, skin and skate vectors, or skate and bone vectors ($p>0.05$). Bone vector rotations correlated negatively with both skin and skate vector rotations, while skin and skate vector rotations correlated positively (Table 8).

Table 8. Paired samples t-test and correlation values for Bone, skin, and skate vectors' rotations from dorsiflexion to neutral position.

	Dorsiflexion to neutral position		
	Bone vs. skin (n = 5)	Skin vs. skate (n = 5)	Skate vs. bone (n = 5)
P	0.59	0.14	0.18
r	-0.48	0.46	-0.64

For plantar flexion, a significant difference existed amongst bone, skin, and skate vector rotations ($p<0.05$ in table 9). The data in the same table also show a negative weak correlation between bone and skin rotations, negative correlation between skin and skate rotations, and a strong positive correlation between skate and bone rotations.

Table 9. Paired samples t-test and correlation values for Bone, skin, and skate vectors' rotations from neutral position to plantar flexion.

	neutral position to plantar flexion		
	Bone vs. skin (n = 5)	Skin vs. skate (n = 5)	Skate vs. bone (n = 5)
P	0.00	0.00	0.00
r	-0.30	-0.51	0.71

Bone, skin, and skate vector rotations across the total motion from dorsiflexion to plantar flexion are shown in table 10. Skin rotations were again the largest and skate rotations the smallest across all subjects except subject 2 whose skate rotation in dorsiflexion was 3.3° higher than his bone rotation. Mean skate rotation was 49% smaller than mean skin rotation and 26% smaller than mean bone rotation, while mean skin rotation was 31% larger than mean bone rotation. Here also the results were systematic

across subjects where skate rotations were about 70% of bone rotations (except for subject 2).

Table 10. Bone, skin, and skate vectors' rotations from dorsiflexion to plantar flexion.

	Dorsiflexion to Plantar flexion (Deg)		
Subject	Bone	Skin	Skate
2	37.27	50.22	39.26
4	34.26	54.57	22.73
5	39.36	52.16	25.49
7	38.28	52.93	25.57
8	40.45	65.53	28.12
Mean	37.92 (2.37)	55.08 (6.04)	28.23 (6.45)

A paired samples t-test showed significant difference ($p<0.05$) amongst bone, skin, and skate rotations (Table 11). There were weak positive correlations between bone and both skin and skate rotations, while skin and skate rotations correlated negatively. Bone, skin, and skate rotations exhibited a similar pattern from dorsiflexion to plantar flexion, however, they differed dramatically in amplitude at plantar flexion especially for skin (Figure 15).

Table 11. Paired samples t-test and correlation values for Bone, skin, and skate vectors' rotations from dorsiflexion to plantar flexion.

	Dorsiflexion to plantar flexion		
	Bone vs. skin (n = 5)	Skin vs. skate (n = 5)	Skate vs. bone (n = 5)
p	0.00	0.00	0.00
r	0.46	-0.24	0.13

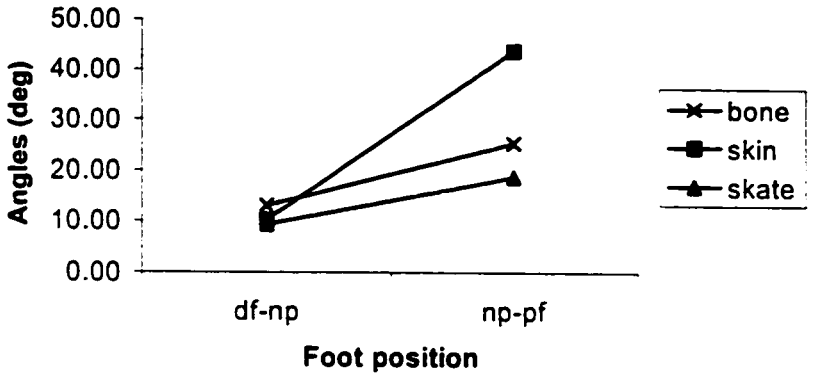

Figure 15. Average bone, skin, and skate vector rotations (x-ray) from dorsiflexion (df) to plantar flexion (pf) through neutral position (np).

On-ice video data

The three-dimensional coordinates of the centroids of the three skate and the three skin markers were calculated in ten frames of the on-ice video views. The frames encompassed a push-off motion from heel-off to toe-off. The distance between the two centroids was determined along the span of the motion. Table 12 shows that the coefficients of variation for the average distance were 12% for subjects 1 and 5 and 20% for subject 6.

Table 12. Average distances between skin and skate centroids from heel-off to toe-off on the on-ice video data.

	Average distance between centroids (cm)		
	Subject		
Frame	1	5	6
1	09.60 (1.74)	10.90 (1.38)	06.00 (0.84)
2	08.70 (1.71)	10.00 (2.47)	06.90 (0.55)
3	09.00 (1.00)	11.20 (2.18)	09.00 (1.21)
4	08.00 (1.34)	11.50 (1.02)	06.50 (2.58)
5	09.70 (1.02)	09.70 (1.22)	10.00 (1.81)
6	07.60 (1.70)	09.70 (2.26)	06.00 (0.58)
7	09.80 (1.82)	07.70 (2.18)	07.00 (2.75)
8	07.40 (1.14)	08.50 (2.43)	05.70 (0.91)
9	10.00 (2.05)	09.70 (1.76)	06.50 (1.36)
10	10.40 (2.69)	10.00 (2.90)	08.30 (2.77)
CV%	11.72	11.79	19.96

Skin and skate vector rotations were calculated from heel-off to toe-off. Table 13 shows that skin rotations were higher or almost equal to skate rotations for all subjects except subject 4. Mean skate rotation was 22% smaller than mean skin rotation. While both types of rotation were highly correlated (r=0.97), the paired samples t-test showed no significant difference between the two (p>0.05). Figure 16 shows the correlation between skin and skate vector rotations on ice.

Table 13. Foot vector rotations (ice) from heel-off to toe-off based on skin and skate markers.

Skin angle difference (heel off-toe off) (deg)				
Subject	Trial 1	Trial 2	Trial 3	Mean
1	53.90	45.10	22.53	40.51
2	30.21	17.92	13.17	20.44
4	10.67	09.75	06.19	08.87
5	35.73	21.94	19.29	25.65
6	30.66	23.27	12.11	22.01
			Mean	23.50
Skate angle difference (heel off-toe off) (deg)				
Subject	Trial 1	Trial 2	Trial 3	Mean
1	25.11	25.00	18.92	23.01
2	22.21	19.86	06.15	16.07
4	18.27	14.55	09.60	14.14
5	22.22	19.03	18.72	19.99
6	27.85	20.72	05.79	18.12
			Mean	18.27
			p (Skin vs. skate) (n = 5)	00.22
			r (Skin vs. skate) (n = 5)	00.97

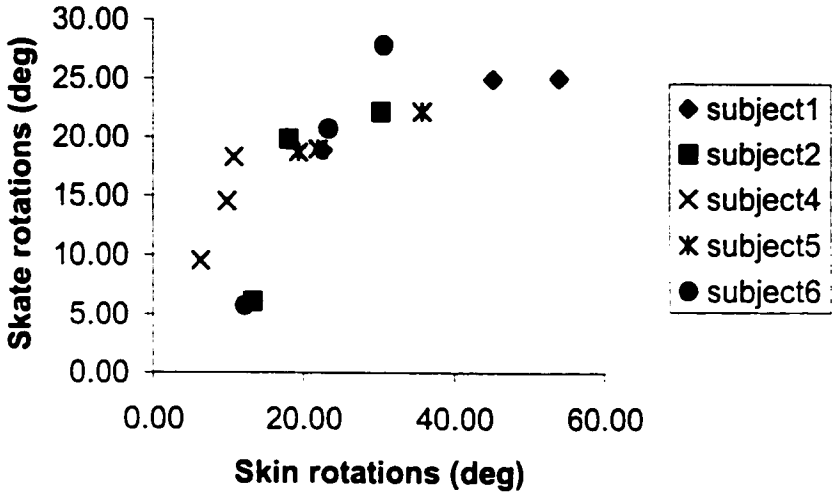

Figure 16. Correlation between skin based and skate based foot rotations (on-ice) from heel-off to toe-off for all subjects.

DISCUSSION

Centroids

If the distance between two points moving in space remained constant, then that means that there is unison in their movement. Therefore, the variation in the distance between different pairs of centroids indicates how the motion of each of the centroids matched the motion of the other. Data from the x-ray part of the experiment (Table 4) show that the distance between bone and skin centroids varied 13% less than the distance between bone and skate centroids, and the distance between skate and bone centroids varied 10% less than the distance between skate and skin centroids (none of the pairs of centroids matched each other closely). This indicates that skin motion is superior to skate motion at representing the trend in bone motion, and the motion of the skate matches the motion of the bone more than it matches the motion of the skin. However, the coefficient of variation value for the distance between skin and skate centroids seen in the x-ray part (36% in table 4) was not seen during actual skating motion; here those values were 12%, 12%, and 20% (Table 12) for subjects 1,5, and 6 respectively. The lower variability of the distance between skin and skate centroids during actual skating is an indication that the coupling of plantar flexion with 45° of external rotation, in the x-ray part, made it a more severe movement than the movement on ice resulting in a large change of the inter-centroid distance. Upon examining the three-dimensional coordinates of the centroids from the x-ray data, as presented in table 6, it is clear that the largest variation in the position of the centroids took place during plantar flexion which was coupled with 45° of external rotation. The position of the skin centroid on the X axis (sagittal plane) varied noticeably less than the position of the bone centroid, and its position on the Y axis

(frontal plane) varied noticeably less than the position of the skate centroid. This indicates that the skin centroid travelled a shorter distance than the other two centroids in both the frontal and sagittal planes and that is due to its location being closest to the axes of rotation of the ankle and subtalar joints.

Inter-centroid distances were larger at dorsiflexion and plantar flexion in comparison to the neutral position. The largest inter-centroid distance was present during plantar flexion because it was a more dynamic motion due its coupling with external rotation. However, the lack of significant difference in the variation of distances between the pairs of centroids indicates the need to measure these distances at a larger number of positions in order to positively discern better and worse matches amongst bone, skin, and skate.

Vector angles

The centroid data was used to describe the pattern of bone, skin, and skate motions and how they relate to each other. However, it did not measure the difference amongst those motions. Therefore, vector rotations were used to determine how much the three types of motion differ from each other. It appears that the motion from dorsiflexion to neutral position was not severe enough to result in a significant difference amongst bone, skin, and skate rotations or to show a regular pattern across all subjects. However, rotations from neutral position to plantar flexion exhibited a regular pattern across all subjects, where skin rotations were the largest and skate rotations were the smallest. Rotation measurements during this part of the motion indicate that skin motion overestimated the underlying bone motion and that skate motion underestimated bone

and skin motions. Furthermore, skate and bone rotations from neutral position to plantar flexion were systematic across all subjects (skate rotations about 70% of bone rotations) except for subject 2. This might suggest the existence of a predictive relationship between the two motions that need to be explored with a larger sample size.

When the total motion of the foot from dorsiflexion to plantar flexion was considered, plantar flexion's effect dominated the total motion in that the skate rotations again underestimated bone and skin rotation. As discussed earlier this underestimation was not seen at dorsiflexion and the dominance of the plantar flexion effect here is due to the larger values of rotation present during this motion. Skin rotations here also overestimated bone rotation as was observed during plantar flexion alone. The similar pattern exhibited by bone, skin, and skate rotations from dorsiflexion to plantar flexion indicates that skate and skin motions could be used as an accurate representation of the trends in bone motion rather than its amplitudes, which differ significantly amongst the three motions.

Skate and skin rotations during actual skating were generally smaller than the rotations during the x-ray part, indicating that none of the subjects went through a full plantar flexion motion between heel-off and toe-off. Except subject 4, all subjects exhibited skate rotations that were equal to or smaller than skin rotations across all trials (trial 2 for subject 2 the difference is only 2°). Skate rotation underestimated skin rotation, however, the lack of sever motion such as full plantar flexion with external rotation resulted in the difference being insignificant. The values exhibited by subject 4 seem to be the result of his skating technique. The video for the subject in question shows

that he did not utilise plantar flexion during push-off; his foot was kept in external rotation and its medial aspect very close to the ice surface for the whole period of push-off. The subject, unlike others, seemed to rely mainly on hip extension as the power generator, which could be due to a larger diameter of the shank, which resulted in the upper aspect of the skate placing higher pressure on the calf muscles and the Achilles tendon limiting the ability to use those muscles to generate plantar flexion.

The results of this study show that skin rotations around the ankle joint significantly overestimate bone rotations by 31%. This overestimation agrees with what is known about skin motion artefact in the literature (Reinschmidt, 1997; Cappozzo et el, 1995; Lafortune et el, 1992). However, it appears to exist only during severe movements such as plantar flexion coupled with external rotation. The results of this study are interesting in relation to skate rotations underestimating bone rotations by 26%, and skin rotations by 49% in x-ray data and by 22% during actual skating. This underestimation did not exist during dorsiflexion and was not significant during actual skating. This finding is the opposite of what is known in the literature about shoe rotations in relation to bone and skin rotations (Reinschmidt, 1997). The difference between shoe and skate movement artefacts could be the result of two reasons; the rigidity of the skate structure which makes it far less flexible than the shoe and the fact that in the Reinschmidt study part of the heel cap of the shoe was removed, increasing the possibility of relative shoe to foot motion. Worth noting is that this study did not consider movements other than plantar/dorsiflexion around the ankle joint complex (in/eversion and ab/adduction), therefore, it is not clear whether the conclusions presented here could also be drawn for all types of movements around the ankle joint complex.

movement artefacts could be the result of two reasons; the rigidity of the skate structure which makes it far less flexible than the shoe and the fact that in the Reinschmidt study part of the heel cap of the shoe was removed, increasing the possibility of relative shoe to foot motion. Worth noting is that this study did not consider movements other than plantar/dorsiflexion around the ankle joint complex (in/eversion and ab/adduction), therefore, it is not clear whether the conclusions presented here could also be drawn for all types of movements around the ankle joint complex.

Sources of error

Some sources of error in this study could not be eliminated or measured. These include errors that might result from the addition of the thermoplastic on top of the skin; although the thermoplastic was very thin (1mm) and had a smooth surface, the interaction between it and the inside of the skate could result in a change in the attitude of skin markers motion. Another source of error in the methodology is the visual determination of the centres of spherical bony structures, the only way to measure this error would be to insert metal markers in the centres of the bones in question and compare their reconstructed coordinates to the coordinates of the visually determined bony centres. The use of one x-ray source that is moved between two positions might also be a source of error that results from the segment moving during the time interval between the two exposures. This error can be eliminated through the use of two x-ray sources that allow for two exposures to take place at the same moment in time. Sources of error in the on ice part of the study could be limited by using a smaller field of view which would require the video cameras to be closer to the filmed segment. This in turn can eliminate marker merging and shadowing problems and permit a clearer view of the small markers.

CONCLUSIONS

The significant difference between skin and bone motions corresponds to the conclusions present in the literature. However, the significant difference between skin and skate motions was present only in the x-ray part of the experiment when the total motion of the foot was considered and the most dramatic change in all three motions took place during plantar flexion that was coupled with 45° of external rotation. The difference between skin and skate rotations during actual skating was not significant. Considering these points, it is clear that the motion performed during the x-ray part was an unrealistic skating motion. The 45° external rotation was added to plantar flexion based on what is called the "Optimal Angle of Propulsion" in the literature. However, this angle, when present in a starting push-off motion, seems to be smaller than 45° and does not continue up to the toe-off part of it. Therefore, based on the results of this study, it can be concluded that, unlike shoe motion, the rigidity of the skate structure results in the skate motion underestimating the motion of the underlying bony and skin structures. However, it is not clear whether this difference exists in movements other than planatr/dorsiflexion around the ankle joint complex. It is also evident from the results that the general pattern of skate motion does accurately represent the pattern of bone and skin motions since the trends of all three motions are similar and a predictive relationship might be present between skate and bone motions. A more representative picture of the difference between the motions in question would be obtained from studying an actual skating motion using fluoroscopy, if expense and logistics allow. Therefore, it is advised that results of kinematic studies of skating based on skate markers be interpreted with caution.

BIBLIOGRAPHY

Allard, P., Cappozzo, A., Lundberg, A., Vaughan, C. L. (1997). Three-dimensional Analysis of Human Locomotion. John Wiley & Sons, Toronto.

Allard, P., Stokes, I., Blanchi, J. (1995). Three Dimensional Analysis of Human Movement. Human Kinetics Publishers, Champaign, IL.

Andre, B., Dansereau, J., Labelle, H. (1994). Optimized vertical stereo based radiographic setup for clinical three-dimensional reconstruction of the human spine. Journal of Biomechanics 27(8), 1023-1035.

Berthonnaud, E., Remy, D., Moyen, B., Carrillon, Y., Dimnet, J. (1998). Inferior limb stereoradiography: technique and applications in clinical practice. http://www.utc.fr/esb/esb98/abs_htm/341.html

Cappozzo, A, Catani, F., and Leardini, A., Benedetti, M.G., and Della Croce, U. (1996) Position and orientation in space of bones during movement: experimental artefacts. *Clin Biomech* 11, 90-100.

Chen, L., Armstrong, C. W., & Raftopoulos, D. D. (1994). An investigation on the accuracy of three-dimensional space reconstruction using the direct linear transformation technique. Journal of Biomechanics, 27(4), 493-500.

Cole, G. K., Nigg, B.M., et al. (1993). Application of the Joint Coordinate System to Three-Dimensional Joint Attitude and Movement Representation: A Standardization Proposal. Journal of Biomechanical Engineering, 115: 344-349.

Crisco III, J.J., Chen, X., Panjabi, M. and Wolfe, S. (1994), Optimal marker placement for calculating the instantaneous center of rotation. Journal of Biomechanics 27(9), 1183-1187.

Dapena, J., Harman, E., Miller, J., (1982). Three-dimensional cinematography with control object of unknown shape. journal of Biomechanics, 15(1), 11-19.

de Koning, J., R. Thomas, et al. (1995). The start in speed skating: from running to gliding. Medicine and science in sports and exercise 29(12): 1703-8.

El Maach, I. (1998). Developpement d'un nouveau systeme pour analyser la biocinematique du genou. Application: Evaluation de l'orthese plantaire. Institut de Genie Biomedical, Ecole Polytechnique de Montreal. Diplome de Maitrise.

Feneis, H., (1981). Anatomicky Obrazovy Slovnik (Anatomical Dictionary). Avicenum, Prague, Czech Republic.

Frankel, V., Nordin, M. (1980). Basic Biomechanics of the Skeletal System. Lea & Febiger, Philadelphia.

Greer, N. (1990). Biomechanics of skating. Winter sports medicine. M. J. Casey. Philadelphia, Davis Co.: 241-247.

Hancock, S. (1999). The influence of three hockey skate boots on the range of motion, elastic moment and stiffness of human ankle joint complex. University of Ottawa, master's thesis.

Hoshizaki, TB., Kirchner, G., Hall, K. Kinematic analysis of the talocrural and subtalar joints during the hockey skating stride in Safety in ice hockey, eds., Castaldi, C.R.and Hoerner, F.E. (1989). ASTM, Philadelphia.

Humble, R. and B. Gastwirth (1988). The biomechanics of forward power skating. Clinics in podiatric medicine and surgery 5(2), 363-76.

Kirchner, G. (1986). A kinematic Description of the Ankle During the Acceleration Phase of Forward Skating. McGill University, master's thesis.

Kwon,Y.H. (1999). Theoretical foundation: DLT method. www.cs.bsu.edu/~ykwon/kown3d/dlt/dlt.htm.

Lafontaine, D., Lamontagne, M. (2000). Development and Validation of a mobile video capture system for spatial kinematics. Proceedings of the XIth Congress of the Canadian Society of Biomechanics, Montreal.

Lafortune, M.A., Lambert, C., and Lake, M. (1992) Skin marker displacement at the knee joint. Proceedings of the Second North American Congress on Biomechanics, Chicago.

Lundberg, A., (1988). Patterns of Motion of the Ankle/Foot Complex. Stockholm, Sweden.

Marino, G. (1977). Kinematics of ice skating at different velocities. Research quarterly 48(1), 93-97.

Marino, G. (1979). Acceleration-time relationship in an ice skating start. Research quarterly 50(1), 55-9.

Marino, G. (1983). Selected mechanical factors associated with acceleration in ice skating. Research quarterly for exercise & sport 54(3), 234-8.

Marino, G. (1984). Analysis of selected factors in the ice skating strides of adolescents. CAHPER journal 50(3), 4-8.

Marino, G., R. Weese, et al. (1979). A kinematic analysis of the ice skating stride. Science in skiing, skating and hockey. J. Terauds. Del Mar, Ca, Academic Publishers: 65-74.

Maslen, B. A., Ackland, T. R. (1994). Radiographic study of skin displacement errors in the foot and ankle during standing. Clinical Biomechanics 9, 291-296.

Minkoff, J., Varlotta, G., Simonson BG., Stone, D.A. Ice hockey in Sports injuries: mechanisms, prevention and treatment, ed., Fu, F.H. (1994). Williams & Wilkins, Baltimore, Md.

Moore, L., (1992a). Clinically Oriented Anatomy (3rd ed.). Williams & Wilkins, Baltimore.

Murphy, N., (1993a). Ankle and Subtalar Joint Three-Dimensional Kinematics Obtained with the Helical Axis Model and Estimated from Talus, Calcaneus and Foot Markers. University of Montreal, unpublished Ph.D. thesis.

Murphy, N., (1988b). Ankle and Subtalar Joint Kinematics: Description Using Stereophotogrammetry. McGill University, Montreal, unpublished master's thesis.

Naud, R. and L. Holt (1980). Comparison of selected stop, reverse and start (SRS) techniques in ice hockey. Canadian Journal of applied sports science 5(2), 94-7.

Nigg, B., G. Cole, et al. (1993.). Effects of arch height of the foot on angular motion of the lower extremities in running. Journal of biomechanics 26(8): 909-916.

Norkin, C.C., Levangie, P. K. (1992). Joint structure and function (2nd, ed.), F. A. Davis Company, Philadelphia.

Pearcy, M. J., (1985). Stereoradiography of lumbar spine motion. Acta Orthopaedica Scandinavica. Supplementum No. 212, 56 : 1-44.

Reinschmidt, C., A. J. van den Bogert, et al. (1997). Tibiofemoral and tibiocalcaneal motion during walking: external vs. skeletal markers. Gait and Posture 6: 98-109.

Reinschmidt, C., A. J. van den Bogert, et al. (1997). Tibiocalcaneal motion during running, measured with external and bone markers. Clinical Biomechanics 12(1), 8-16.

Reinschmidt, C., A. J. van den Bogert, et al. (1997). Effect of Skin Movement on the Analysis of Skeletal Knee Joint Motion during Running. Journal of Biomechanics 30(7), 729-732.

Rockar, P., (1995). The Subtalar Joint: Anatomy and Joint Motion. Journal of Orthopaedic and Sport Physical Therapy 21(6), 361-372.

Rosenfeld, L. B., Ronsky, J., Wiley, P., Caswell, D. (1999). Functionality of a new system of calcaneal marker attachment used to collect three dimensional kinematic data both shod and barefoot. Procedures of the XVIIth Congress of the International Society of Biomechanics, Calgary.

Roy, B. (1977). Biomechanical features of different starting positions and skating strides in ice hockey. Biomechanics_V1-B. E. Asmussen and K. Jorgensen. Baltimore, University Park Press: 137-141.

Sangeorzan, B.,Subtalar Joint: Morphology and Functional Anatomy in Inman's Joints of the Ankle, ed. Stiehl, J.,(1991).William & Wilkins, Baltimore.

Shapiro, R., (1978). Direct Linear Transformation Method for three-dimensional Cinematography. The Research Quarterly 49(2), 197-205.

Siegler, S., Chen, J., Schneck, CD., (1988). The three-dimensional kinematics and flexibility characteristics of the human ankle and subtalar joints--Part I: Kinematics. Journal of Biomechanical Engineering 110(4), 364-73.

Tortora, G., (1998, 8th ed.). Principles of Human Anatomy, Benjamin/Cummings Science Publishing.

Van Ingen Schenau, G., R. De Boer, et al. (1989). Biomechanics of speed skating. Biomechanics of sport. C. L. Vaughan. Boca Raton, CRC Press: 121-167.

Van Ingen Shenau, G. J. and B. K. (1980). Biomechanical model of speed skating. Journal of human movement studies 6(1), 1-18.

Zatsiorsky, V. (1998). Kinematics of Human Motion. Human Kinetics, Champaign, IL.

Appendices

Appendix (A)

Calculations of the centroid of three points in space

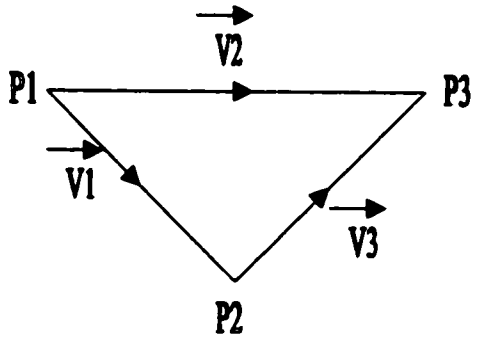

$P1 = (a1, a2, a3)$
$P2 = (b1, b2, b3)$
$P3 = (c1, c2, c3)$

$\vec{V}1 = P1P2 = (b1, b2, b3) - (a1, a2, a3) = (b1 - a1, b2 - a2, b3 - a3) = (X1, Y1, Z1)$
$\vec{V}2 = P1P3 = (c1, c2, c3) - (a1, a2, a3) = (c1 - a1, c2 - a2, c3 - a3) = (X2, Y2, Z2)$
$\vec{V}3 = P2P3 = (c1, c2, c3) - (b1, b2, b3) = (c1 - b1, c2 - b2, c3 - b3) = (X3, Y3, Z3)$

$l1 = P1 + t(\vec{V}1 + \vec{V}2)$
$X = a1 + t(X1 + Y2)$
$Y = a2 + t(Y1 + Y2)$
$Z = a3 + t(Z1 + Z2)$

$l2 = P2 + s(-\vec{V}1 + \vec{V}3)$
$X = b1 + s(-X1 + X3)$
$Y = b2 + s(-Y1 + Y3)$
$Z = b3 + s(-Z1 + Z3)$
$X : a1 + (X1 + X2) = b1 + s(-X1 + X3)$
$Y : a2 + t(Y1 + Y2) = b2 + s(-Y1 + Y3) \Rightarrow \dfrac{a2 - b2 + t(Y1 + Y2)}{(-Y1 + Y3)} = s$

Substitution :

$$a1 + t(X1 + X2) = b1 + \frac{(a2 - b2 + t(Y1 + Y2)(-X1 + X3)}{(-Y1 + Y3)}$$

$$a1(-Y1 + Y3) + t(X1 + X2)(-Y1 + Y2) = b1(-Y1 + Y3) + (a2 - b2)(-X1 + X3) + t(Y1 + Y2)(-X1 = X3)$$

$$t = \frac{b1(-Y1 + Y3) + (a2 - b2)(-X1 + X3) - a1(-Y1 + Y3)}{(X1 + X2)(-Y1 + Y2) - (Y1 + Y2)(-X1 + X3)}$$

$X = a1 + t(X1 + X2)$
$Y = a2 + t(Y1 + Y2)$
$Z = a3 + t(Z1 + Z2)$

Appendix (B)

Calculation of Vector Angles
(Vector Cross-product)

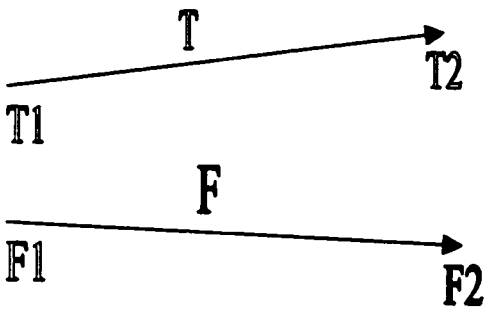

$$|T| = \sqrt{Tx^2 + Ty^2 + Tz}$$

$$|F| = \sqrt{Fx^2 + Fy^2 + Fz^2}$$

Total angle:

$$\overline{T} * \overline{F} = |T| * |F| * \cos\alpha$$

$$\overline{T} = (Tx, Ty, Tz)$$

$$\overline{F} = (Fx, Fy, Fz)$$

$$(Tx, Ty, Tz) * (Fx, Fy, Fz) = |T| * |F| * \cos\alpha$$

$$\cos\alpha = \frac{(TxFx + TyFy + TzFz)}{|T| * |F|} \Rightarrow \alpha = \arccos\frac{T * F}{|T| * |F|}$$

Appendix (C)
Three-dimensional coordinates of individual markers (x-ray)

Bone

		marker1			marker2			marker3		
		X	Y	Z	X	Y	Z	X	Y	Z
Dorsiflexion	subject2	30.00	24.86	-30.05	31.18	27.48	-32.33	34.30	26.45	-33.31
	subject4	30.58	22.03	-29.94	31.90	25.65	-32.97	34.52	23.63	-33.56
	subject5	31.33	24.18	-28.96	32.36	25.20	-31.91	34.80	25.64	-32.32
	subject7	30.34	23.82	-29.58	31.35	26.67	-32.31	33.85	25.03	-32.66
	subject8	30.26	24.11	-30.36	31.34	27.09	-33.07	33.80	25.04	-33.63

		marker1			marker2			marker3		
		X	Y	Z	X	Y	Z	X	Y	Z
Neutral	subject2	26.85	23.20	-30.89	27.39	25.27	-33.53	30.11	24.20	-34.86
	subject4	27.95	23.16	-30.75	28.59	24.31	-33.88	31.12	23.91	-35.00
	subject5	28.30	24.01	-30.10	28.77	25.84	-32.92	31.09	26.50	-33.73
	subject7	28.34	23.78	-30.28	29.16	25.73	-33.19	31.51	25.07	-33.86
	subject8	27.72	23.07	-31.17	28.35	25.28	-34.03	31.02	25.45	-34.61

		marker1			marker2			marker3		
		X	Y	Z	X	Y	Z	X	Y	Z
Plantar flexion	subject2	25.00	19.98	-30.89	24.20	23.91	-33.46	24.94	22.38	-35.88
	subject4	27.21	20.99	-30.48	26.51	23.51	-34.14	27.32	22.73	-35.80
	subject5	25.48	23.37	-30.66	24.62	25.80	-33.55	26.14	25.91	-35.11
	subject7	25.78	21.55	-30.74	24.43	23.38	-34.24	26.14	22.92	-35.62
	subject8	24.18	21.30	-31.36	22.95	23.84	-34.30	24.71	25.19	-35.72

Skin

		marker1			marker2			marker3		
		X	Y	Z	X	Y	Z	X	Y	Z
Dorsiflexion	subject2	33.99	20.57	-26.84	34.00	20.61	-30.83	37.63	22.65	-28.77
	subject4	35.15	18.31	-26.87	34.59	17.75	-30.08	38.41	19.00	-28.67
	subject5	33.91	19.73	-27.92	33.79	19.35	-30.70	37.66	20.73	-29.10
	subject7	34.78	19.30	-27.75	34.41	19.34	-31.33	37.96	20.99	-29.78
	subject8	33.64	19.81	-28.60	33.56	19.96	-30.99	37.75	20.94	-30.11

		marker1			marker2			marker3		
		X	Y	Z	X	Y	Z	X	Y	Z
Neutral	subject2	31.48	19.04	-28.73	30.76	18.61	-32.53	34.45	20.02	-31.44
	subject4	32.96	18.41	-28.63	31.73	18.03	-31.70	35.79	19.16	-30.94
	subject5	31.06	19.35	-29.84	30.47	19.36	-32.34	34.61	20.62	-31.47
	subject7	33.12	20.61	-28.98	32.34	20.53	-32.58	36.08	22.30	-31.36
	subject8	31.16	18.67	-29.87	30.71	18.82	-32.22	34.94	19.00	-32.05

		marker1			marker2			marker3		
		X	Y	Z	X	Y	Z	X	Y	Z
Plantar flexion	subject2	29.79	20.55	-30.18	28.53	19.39	-33.47	30.57	22.17	-33.59
	subject4	32.12	22.47	-28.97	31.41	20.40	-31.60	33.50	23.80	-31.88
	subject5	30.96	21.70	-30.90	30.34	20.63	-33.20	32.52	23.99	-33.33
	subject7	32.30	20.81	-29.95	31.47	19.14	-33.11	33.35	23.09	-33.41
	subject8	30.25	21.12	-30.68	29.42	20.05	-32.93	32.35	23.96	-33.63

Skate

		marker1			marker2			marker3		
		X	Y	Z	X	Y	Z	X	Y	Z
Dorsiflexion	subject2	23.44	19.43	-27.61	28.90	20.63	-28.42	32.04	21.68	-33.28
	subject4	24.95	18.38	-26.54	29.46	18.30	-28.77	33.08	18.80	-32.57
	subject5	24.69	19.41	-27.59	29.78	20.04	-29.08	32.61	21.51	-33.42
	subject7	25.14	19.40	-28.26	29.69	19.84	-29.47	32.56	20.24	-33.75
	subject8	24.49	19.65	-27.90	29.61	20.14	-29.49	32.38	20.72	-33.86

		marker1			marker2			marker3		
		X	Y	Z	X	Y	Z	X	Y	Z
Neutral	subject2	21.24	19.51	-27.00	26.35	19.50	-29.13	28.41	20.29	-34.43
	subject4	22.92	18.11	-26.53	26.92	18.50	-29.50	29.85	18.29	-33.90
	subject5	22.21	19.44	-27.88	26.94	19.92	-30.20	29.09	20.51	-34.87
	subject7	23.47	20.18	-28.35	27.84	20.85	-30.15	30.19	21.67	-34.70
	subject8	22.32	19.25	-27.84	27.11	19.49	-30.13	29.25	19.67	-34.83

		marker1			marker2			marker3		
		X	Y	Z	X	Y	Z	X	Y	Z
Plantar flexion	subject2	22.50	16.25	-25.20	25.64	18.59	-28.93	27.69	19.51	-34.97
	subject4	23.93	16.29	-24.92	26.67	18.36	-28.64	28.78	19.81	-33.45
	subject5	24.77	17.45	-26.95	27.62	19.76	-30.38	28.29	20.48	-35.42
	subject7	25.48	15.49	-26.74	28.22	17.61	-29.74	29.30	17.63	-34.75
	subject8	23.99	14.99	-26.93	26.83	18.49	-30.15	27.42	19.31	-35.14